Study of Band Gap of Zinc Oxide (ZnO) with Inclusion of MoS_2 and Its Use as Electron Transport Layer in Organic Photovoltaic

Amir Khalid

NUST201362324MSCME67713F

This work is submitted as a MS thesis in partial fulfillment of the requirement for the degree of

(MS in Materials and Surface Engineering)

Supervisor: Dr. Amir Habib

School of Chemical and Materials Engineering (SCME)
National University of Science and Technology (NUST)
H-12, Islamabad, Pakistan.

ACKNOWLEDGEMENT

'Behold! In the creation of the skies and the earth and the alternation of night and day there are indeed signs for men of understanding.' [Quran, 2:164]

All the praise to Allah Almighty without whom nothing is possible in the world. Special gratitude to the honourable, Dr. Amir Habib, thesis supervisor, for encouragement, appreciation, precious time, treasured instructions and guidelines throughout the research work.

Also special thanks to Maj. Imran Ahmad and Mohammad Noman Amin for their help, valuable instructions and guidance all through my research work. And also gratitude to all my teacher who taught the course work, my class mates for valued discussions and support.

And finally, very special acknowledgement for the commitment of my family especially my mother and brother towards me, whom love, encouragement and support in all aspects of my life made it possible for me to be at this position.

Amir Khalid

DEDICATION

To those whom I owe my breath.

ABSTRACT

In renewable energy, solar cell is very actively investigated topic now a days because of sun as limitless source of energy. Among solar cells, organic solar cells are of major focus because of their future possibilities and potential towards cheap and efficient solar devices. Organic photovoltaic (OPV) are devices based on the organic-inorganic interface which use P3HT: PCBM as active layer and metal oxides as electron transport layer. The materials selected are because of the good optical properties, good extinction coefficient, chemical stability, charge mobility and nontoxicity.

ZnO a wide band gap semiconductor is used as electron transport layer due to its good electron mobility. Its band gap lies in ultra violet range which if further reduced the material will fall in the higher wavelength visible range effecting both light harvesting by the devices and enhancing exciton disassociation and extraction. In this work Molybdenum di-sulphide MoS_2, a low band gap two dimensional material is used for the band gap engineering of ZnO and its effects are studied on the current Isc, current density Jsc and fill factor.

Band gap of ZnO was reduced from 3.34eV to 2.92 eV. UV-Vis spectroscopy and cyclic voltammetry techniques were used to verify the reduction in band gap, results obtained by both techniques in agreement with each other with in the limits of experimental errors. XRD results confirmed the imbedding of MoS_2 in ZnO thin films. Also SEM and AFM images of ZnO films verified very fine nano-particles, and images of exfoliated MoS_2 showed very few layers of MoS_2 of thickness 0.939 nm. The Fill factor and short circuit current showed increasing trends due to increasing MoS_2 concentration in ZnO thin films reflective of increase in electron mobility due to incorporation of MoS_2. Based on these results ZnO-MoS_2 composite can be an efficient electron transport material for use in thin film photovoltaics.

Table of Contents

List of Figures

List of Tables

List of Abbreviations

PCE	Power conversion efficiency
FF	Fill factor
1G	First generation solar cell
2G	Second generation solar cell
3G	Third generation solar cell
PV	Photovoltaic
HOMO	Highest occupied molecular orbit
LUMO	Lowest unoccupied molecular orbit
XRD	X-ray diffraction
OPV	Organic photovoltaic device
SEM	Scanning electron microscope
AFM	Atomic force microscopy
CV	Cyclic Voltammetry
I-V	Current-Voltage
CVD	Chemical vapor deposition
ITO	Indium Tin oxide

Chapter 1

Introduction

1.1 Motivation

Whole world is moving toward renewable energy sources and research in this field is more focused for last two decade. Why renewable energy? Most of the world energy depends, now a day, on the fossil fuels and nuclear power and firstly both of these are environmental unfriendly. Fossil fuel are causing major problems like global warming and raising sea levels dramatically by producing CO_2 and sources underground are depleting more rapidly as the population is increasing. While nuclear fission waste disposal, radiation poisoning and cost are major setbacks of this kind. It is not reliable, difficult to control and contain in case of natural disaster or possible safety protocol failure.

Due to this, developed countries are shifting towards more renewable energy sources which are superior in many ways like nonhazardous, environmental friendly, no CO_2 emissions, and long life and mostly depends upon sources which are non-depleting relative to Carbon based fuels.

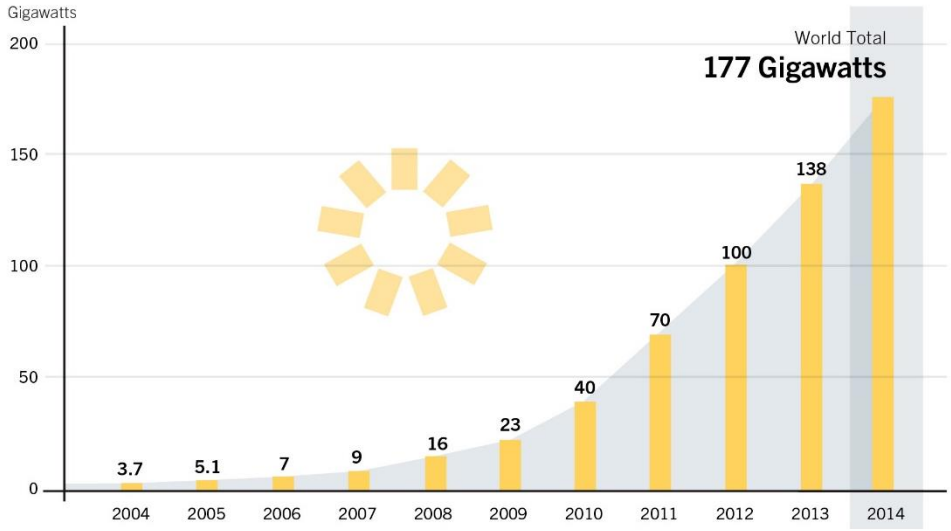

Figure 1-1-1 Solar PV capacity, 2004-2014 [1]

Renewable energy sources cover every non carbonaceous and limitless source usually include solar energy, tidal energy, wind power, hydro-electric energy, biomass and geo thermal energy sources. From all of above solar power is considered the future of energy system as many

proposition and innovations in this regard are made such as solar satellites, solar hydroelectric power plants (SHE) and concentrating solar power (CSP).

From all the energy consumed around the globe, the lowest of energy comes from renewable sources that is 0.5% of the total production. Total energy consumption in 2050 is estimated to be 30 TW, which was 13 TW in 2003. According to the projections, 2 billion have still no electricity. All the industrialized civilizations are more and more depending upon solar energy, at the end of 2014 about 1 percent of total world electricity is produced viva solar energy which is 178GW of total. Germany alone produces 38.2 GW electricity from solar source highest of all countries.[2]

That's why solar cell technology is more and more focused in most research groups working all around the globe. Science behind solar energy is that light inform of photons is directly converted into electrons (electric charge) with help of using photo voltaic (PV) cells. The major objective of device is to absorb as much light as it can and convert it. Silicon based devices are commercially available and Si is used currently for solar cell fabrication. Organic and hybrid materials are used for low cost photovoltaic devices fabrication as better substitute to Si based inorganic cells which are expensive. Organic and Inorganic PV devices are in focus and are showing promising results. Design of a photovoltaic device requires to absorb maximum sun light and convert most of it to electric current for best output.

Development in field of nanotechnology is playing vital role in latest research for increasing the efficiencies, reliability, stability and life. The increase in surface to the volume ratio, interface, efficient charge transfer, size reduction, and developments in 2 dimensional materials with superior properties of strength, charge transfer, band gap and conduction has revolutionized the field of hybrid photovoltaic. The nanotechnology spectrum tells how we convert sunlight and how it is utilized. The photovoltaic converts solar energy into electric energy, and further use of electrochemical energy converted from electric energy in batteries, capacitors and photonics. The use of thermos photovoltaic and thermoelectricity produce from thermal energy and converted from solar to thermal energy. And the Chemical energy converted from solar energy is used in photo catalysis and further used in fuel cells for production of bio fuels and hydrogen.

1.2 Brief Overview

Solar cells are of three generations which are silicon based 1st generation solar cell, thin film 2nd generation solar cells, and then the hybrid 3rd generation solar cells. The power conversion efficiencies of 1st generation and 2nd generation is better but are not beneficial in sense of manufacturing process, the availability of their raw materials and high capital cost. The 3rd generation solar devices developed with help of nanotechnology are optimized, which are under process in research phase with very few commercialized products. Previously carbon nanotubes were used for supporting electron mobility but resent developments in the 2D materials sometime referred as "single layer materials" such as graphene, MoS_2, borophene, silicene etc, now these have shown promising results when used give cheap devices who has better electron conductivity and are simple to synthesis than nano-tubes. The solar cells based on nanotechnology are of many types such as Schottky solar cell, dot sensitized solar devices, depleted heterojunction devices, dye sensitized devices, hybrid solar cell quantum. These types of solar devices have some problems in terms of synthesis, expenses, stability and life but still polymer photovoltaic cell is the cheapest one.[3, 4]

For the objective of effective hybrid solar cells, device is fabricated from small and direct band gap offering materials. Important point is that these materials can spread over a large area, give the device of considerably higher power conversion efficiency (PCE) and stability for the resulting devices. To meet the specs, a broad range of photovoltaic devices are proposed and reported. Among others, many efforts have been made to optimize the ZnO thin films used as electron transport layer. ZnO thins film are optimized before by using graphene which lowers the band gap considerably.

The most widely studied OPV devices in combination with ZnO are poly 3-hexylthiophene (P3HT): phenyl- C61- butyric acid methyl ester (PCBM) / poly p- phenyl-enevinylene (PPV) blended bulk heterojunction (BHJ), this is due to excellent charge transport and perfectly matching band gap. However, in P3HT: PCBM cell, PCBM an acceptor material has high volume ratios than the donor material i.e. P3HT in this case. The volume ratio of P3HT: PCBM (33:66) and the weight ratio (1:0.8) is successful in device fabrication. In these devices, P3HT cover less area which is donor as compared to acceptor (PCBM) which occupies more, this restricts the generation of maximum charge carriers and thus the efficiency of PV device is lower. PCBM is an expensive material to be used. By introducing metal oxide as an acceptor material which would occupy a comparable cell area along with donor P3HT.

In hybrid solar devices, generation of charge and separation occur at the same time on the material interface. The exciton cells developed has a disadvantage that is at nano scales the materials properties becomes critical and the large interfacial area in these nano structured devices could causes the recombination and trapping of charges at the interfaces which reduces the power conversion efficiency of these device. This problem need to be addressed to make the hybrid solar cell efficient and make it commercially viable.

The charge transport properties in excitonic devices and catalysts can be improved by utilizing mixture of carbonaceous materials like C60 fullerenes and Carbon Nanotubes. These material composites show reduced recombination of charges with enhanced current generation and activity in visible light range. The interaction and integration of carbon materials in these system greatly affect the photocatalytic semiconductors.

Monolayer MoS_2 possesses enhanced properties such as better transparency, conductivity and much larger surface area. The photocatalytic behaviour of semiconductors is effected positively by these properties. In this research project we will first fabricate and characterize the nanostructures in thin films of Zinc Oxide (ZnO), then MoS_2 is exfoliated and characterize and then added to ZnO to investigate its effect on the photocatalysis of ZnO thin films. These thin films will be further utilized in the fabrication of hybrid solar cells.

1.3 Outlines of the Research Work:

The purpose of this research work is to reduce the band gap of ZnO thin film by inclusion of exfoliated MoS_2 which will help electron transport layer to reduce its band gap due to low band gap of monolayers MoS_2 in hybrid solar cell.

- For this first Molybdenum disulphide MoS_2 powder is to be exfoliated via liquid phase exfoliation for purpose of attaining exfoliated MoS_2.
- ZnO sol is prepared and characterized for better understanding. Different compositions of ZnO thin films with exfoliated MoS_2 are prepared and characterized.
- Finally hybrid solar cells are fabricated and tested, the results are finally compiled.

Chapter 2

Literature Review

2.1 Solar Cell:

A solar cell is the device which converts solar energy directly into electric current. This require photo sensitive material which when exposed to sunlight receives its photon and convert into exciton (an electron-hole pair), this layer produces both current and voltage by raising the electron to a higher energy state so that it could have enough energy to go into outer circuit. In the external circuit the electron losses its energy and go back to active layer. Numerous processes and materials are available and studied for the prerequisites considered for photovoltaic energy conversion, semiconductor metal oxide materials are widely used in the form of a *p-n* junction.

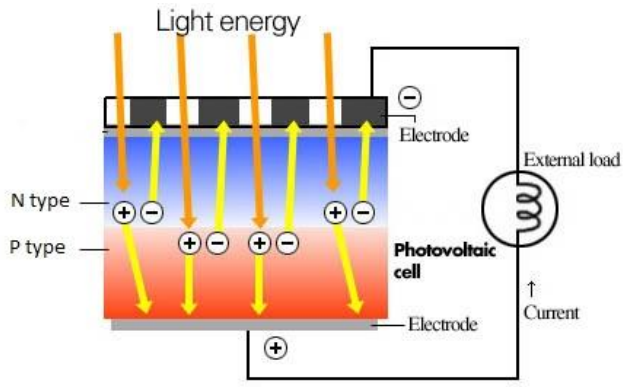

Figure 2-1 A general photovoltaic cell

2.2 Solar Cell Classifications:

Solar cell are classified in four main categories called generations.

2.2.1 First Generation Solar Cells:

1st generation cells consists of Germanium or Silicon which are doped with Boron and Phosphorus in a p-n junction. This generation solar panels are dominating commercial markets now a days. Solar cells falling in this generation are relatively expensive in production but have low efficiencies. Silicon cells have a potential of quite high efficiencies but for this very pure

silicon is required, and due to the energy-requiring processes, the prices are too high in comparison with the power output. Single crystal Silicon solar cell can have the efficiency of up to 25%.[5]

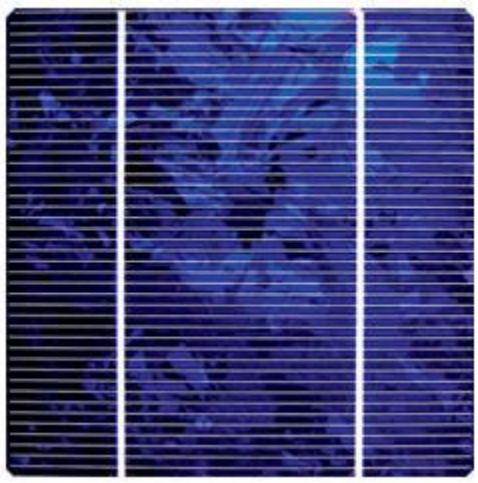

Figure 2-2 Multi-crystalline Silicon Cell Panel[5]

2.2.2 Second Generation Solar Cell:

The second generation (2G) solar cell applies amorphous, proto-crystalline, and nano-crystalline to plastic and over metal surface by chemical vapour deposition. Amorphous silicon, Cu (In,Ga)Se_2 and CdS/ CdTe based photovoltaic are fabricated by physical vapour deposition, sputtering and plasma enhanced chemical vapour deposition. These 2^{nd} generation cell have efficiencies less than the crystalline silicon PV and also have lower production cost. Scientists moved from First generation to thin film solar cells in opposition to high cost of wafer silicon also called crystalline silicon due to high cost which are commercially not feasible. Overall thin film (2G) solar cells are less expensive and have lower efficiencies than crystalline silicon cells. Most thin film cell have efficiencies of 12-20% while prototype efficiency from 7-13% and commercial product efficiency of 9%. Thin film devices can have the efficiency of 10-16%, with the best reported efficiency of 18%.

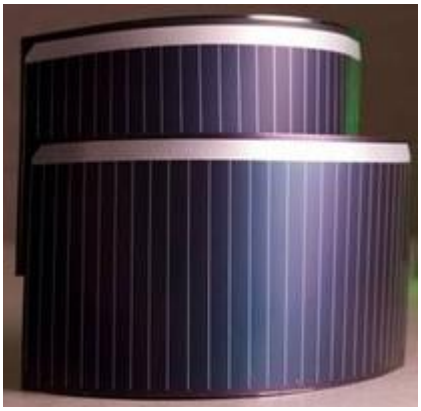

Figure 2-3 Flexible Copper Indium Gallium di-Selenide solar cells [5]

2.2.3 Third Generation Solar Cells:

3rd generation Photo Voltaic technologies use conductive, organic polymers or small molecules for sunlight absorption and electric charge transfer. Its advantages are low cost of manufacturing and flexible large scale production capabilities. These assorted design 3G cell comprises of organic photo-voltaic OPV, dye sensitized solar cells (DSSCs) and multi-junction solar devices. Both DSCs and OPVs have relatively lower PCE; the highest reported PCEs for these devices are 8.3% and10.4% respectively. Cheap materials and low processing costs could compensate for the unfavourable PCE.[5]

For increasing the power to cost ratio of multi-junction solar cells efforts must be in increasing efficiency. In structure third generation solar cells are actually few layers of different material with varying properties stacked on top of one another. Each semiconductor in the layer has a unique band gap which help in increasing the band of the solar spectrum that the PV can absorb. Layers of cells absorbing in the solar spectrum range can surpass the Shockley and Queisser limit, the theoretical efficiency limit that reaches 66%. In labs, highly efficient solar devices fabricated which are layered triple-junction photovoltaics which gives PCE as high as 40%.

3G also covers high cost and high performance experimental multi-junction solar cells which in solar cell performance holds the world record. This type has commercial applications only to some extent because of the expensive production. A new class of thin film photo voltaic cells currently under investigation are perovskite solar cells. On other hand, plastic photovoltaic or polymer solar cells, have several benefits like simple, quick and inexpensive large scale production and readily available material for use that are also potentially cheap. Plastic solar cells can be synthesized with industrial roll-to-roll R2R technology that is same as paper printer. Although the stability and performance of 3rd generation solar cells is still

limited in comparison with 1st and 2nd generation solar devices but they possess great potential and 3G are already commercialized for example infinitypv.com.[3]

2.2.4 Fourth Generation Solar Cells:

4th generation solar cells are actually based on 'organics-in-organics'. They offer enhanced PCE as compared to current 3rd generation solar cells.4th generation brings together the flexibility of polymer thin films and low cost with the more stable of new inorganic nano-structures thin film for enhancing the optoelectronic properties of PVs. The device designs are for the purpose of improving the inexpensive nature of PV device structure by adopting the solution process-able techniques and by joining inorganic components to enhance charge transport, the charge dissociation and energy harvesting cross-sections within the PV cells.[6]

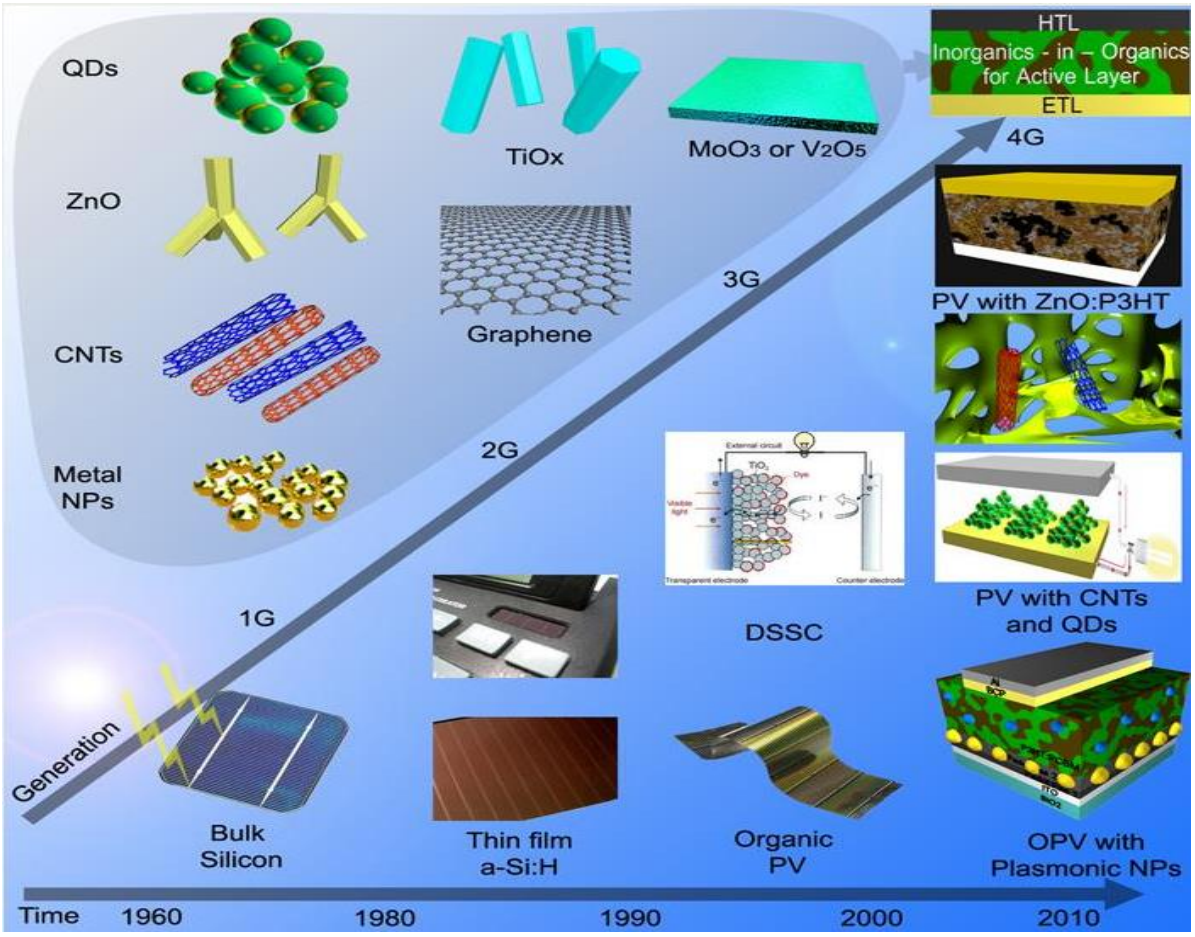

Figure 2-4 Timeline of different generations of solar cells and the developments with time from 1st generation (1G) to 4th generation (4G), with associated nanomaterial constituents.[6]

2.3 Hybrid Photovoltaic Device Structure:

The synthesised hybrid solar cells is same as, in terms of layers, organic solar cells, the one dissimilarity is replacement of organic electron accepting layer by inorganic nanoparticles. The nanoparticles used are in the form of nano-rods, nanowires or quantum dots. [7]

The two types of organic photovoltaics are:

- Normal OPV
- Inverted OPV

2.3.1 Normal OPV:

In a normal solar cell, most of charge carriers are generated close to the anode, such that in comparison to holes, electrons have to travel much longer distance to reach cathode [8]. The device is fabricated on a clean glass substrate and anode is a semi-transparent oxide part, usually coated glass by indium tin oxide (ITO). The function of ITO is to successfully transmit light through without absorbing and reflecting, and should collect holes from the system. PEDOT–PSS a conductive polymer mixture is often placed between anode and photoactive layer for improving hole collection. A thin layer of PEDOT–PSS is deposited by spin coat on to ITO coated glass. PEDOT–PSS coated layer have benefits such as efficient hole transporting layer and exciton block layer, it protects the active layer from oxygen, smooth the ITO surface and stops the electrons from diffusing into the active layer, which can cause to undesirable trap sites.[7] The donor and acceptor material are in photoactive light absorbing layer. Active layer is sandwiched between anode and cathode. Several synthetic techniques are used to spread the inorganic acceptor. Aluminium cathode is deposited, although gold, calcium or magnesium minerals may also be used. Cathode function is to collect electrons from the active layer. Thermal evaporation is used from cathode deposition. The light is illuminated through the glass substrate in normal OPVs.

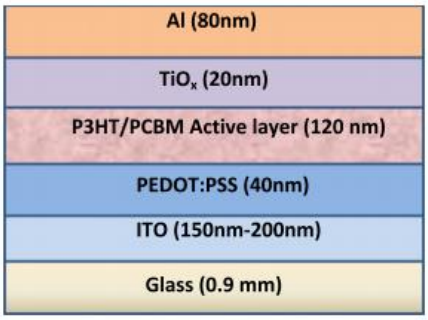

Figure 2-5 Schematic diagram of regular hybrid solar cell [7]

2.3.2 Inverted OPV:

In inverted solar devices, electron travel shorter distance as excitons are generated close to cathode and the holes have to travel longer distance.[8] The PEDOT: PSS has acidic characteristics which cause serious issues at ITO interface about device stability and that's why a deposited high work function metal electrodes are getting attention. Due to such problems, a novel structure, where the charge selection characteristics are reversed, such structure is inverted OPV. Electrons flow towards transparent electrode from back electrode. This structure gives device stability. In inverted solar device, a top metal electrode have high work function which reverse the charge carrier collection polarity and also air sensitivity of cell is reduced. The novel inverted OPV framework have high work function top electrode of metal oxide or metal [8]. In the case of an inverted device structure, on top of the ITO layer, as transparent cathode a 20 nm thick layer of zinc oxide (ZnO) is used, then a layer of the polymer fullerene bulk heterojunction blend P3HT: PCBM as active layer is applied and a thick layer of PEDOT:PSS as transparent anode which is covered with a 100 nm thick Al layer (electrode) as electric contact is used [8]. Others like Ag, Cu, and Au can be used as anode contact. In normal OPV, the issue of degrading and efficiency reduction due to acidic behaviour of PSS due to deposition of PEDOT: PSS over ITO coated glass. That's why we are using inverted solar cell in this research work.

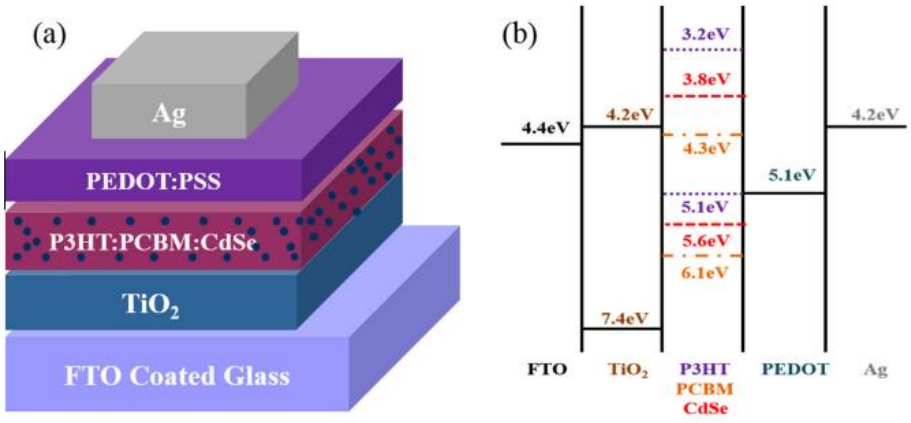

Figure 2-6 (a) Inverted hybrid solar cell schematic. (b) Energy band diagram of the inverted OPV [8]

Following are the I-V characteristics curve for regular OPV and inverted OPV, graph shows that inverted OPV has more open circuit voltage and less current than normal OPV in figure. 2-7

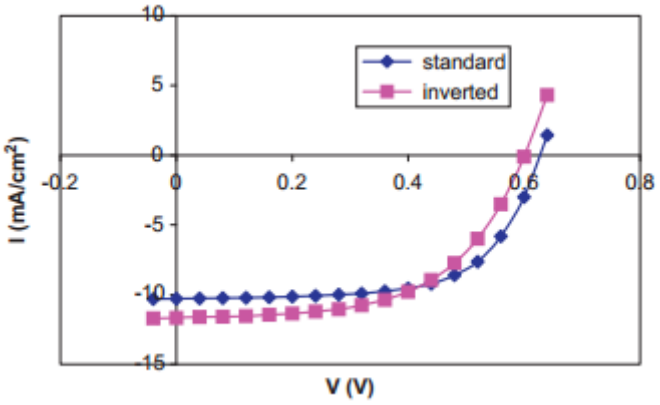

Figure 2-7 . I-V characteristics curve of normal OPV and inverted OPV

Table 2-1 Comparison of Normal and Inverted OPV

Cell structure	V_{oc} (mV)	I_{sc} (mA/cm^2)	FF	PCE (%)	Mobility (cm^{2}V^{-1}s^{-1})
Normal cell	620	10.2	0.64	4.05	4.6×10^{-3}
Inverted cell	594	11.6	0.57	3.90	3.8×10^{-3}

2.4 Photovoltaic Device Operation and Working Principle:

Different steps in production of electric current from photon are as follow

- **Photon absorption**: Receiving of sunlight (photon) by the active region of device and formation of exciton (electron-hole pair).
- **Exciton diffusion**: Movement of exciton to the outer edge of active layer at donor acceptor interface
- **Charge separation**: electron hole separation occurs and electron is received by electron transport layer (acceptor) from where it moves to the external circuit by passing through cathode.
- **Charge transport and collection**: While hole travels to electron transport layer which is connected to electrode (anode) of solar cell.[1]

2.4.1 Exciton Generation and Movement:

The operating mechanism of OPV differs from silicon based solar devices, this difference is because of the organic semiconductors fundamental properties to their inorganic alternatives. When light falls on the photoactive region of device, electron in the valence band is excited to conduction band, this produce an electron-hole pair also known as 'exciton'. Exciton is generated in donor part of the material which dissociates itself at the donor acceptor (D–A) interface.[9]

Figure 2-8 (a) is showing the energy band diagram where acceptor material's conduction band and LUMO of donor's energy level offset provides the necessary force to overcome the exciton binding energy, i.e. ΔE_{ES}. ΔE_{ES} the excited state energy help dissociating electron-hole pair. When the exciton is generated in the acceptor region than the acceptor's valance band edge is considered and the donor material's energy offset of HOMO is required for successful dissociation of exciton at donor acceptor interface. Now the energy offset is denoted as ΔE_{GS} which is ground state energy offset. The exciton dissociation at the donor acceptor phase is due to energy offsets at the interface, therefore the material combination in active layer should be in agreement for successful charge dissociation in the system. Most important factor which has direct relationship with charge dissociation is the interfacial area. Bulk heterojunction devices have such structures with maximum interfacial area between well combined donor and acceptor.[10]

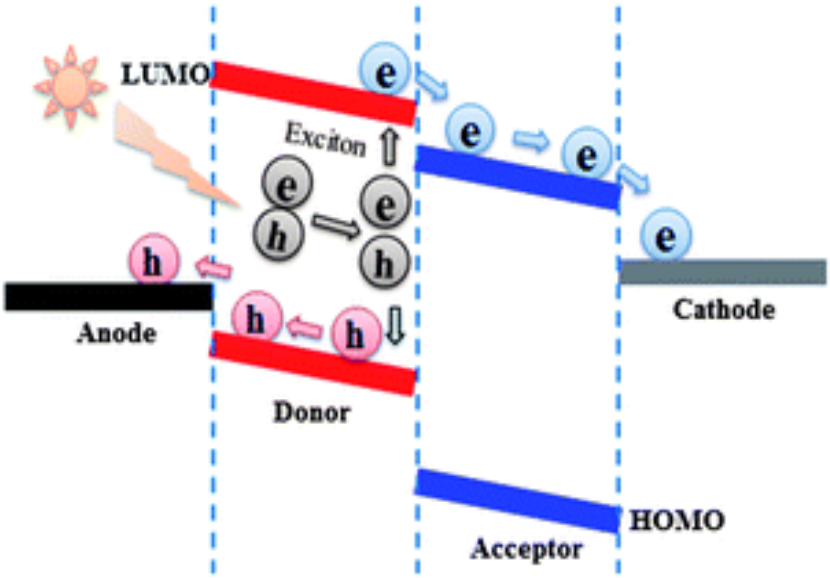

Figure 2-8 Exciton absorption and charge movement in cell [11]

A comparison can be made from Fig.2-8 (b), (c) of two different heterojunction structures. The major difference between the two is the interfacial area between donor and acceptor which changes the diffusion length of the charge carrier. Fig. 2-8(b) shows the bulk heterojunction system having small diffusion length and large interfacial area which maximise the exciton dissociation yield. This develops efficient conductive paths and close distribution of phases through these charges (electrons, hole) transfer is efficient. Thus the conclusion is that donor and acceptor arrangement in the active layer is of great importance for improved performance.[12]

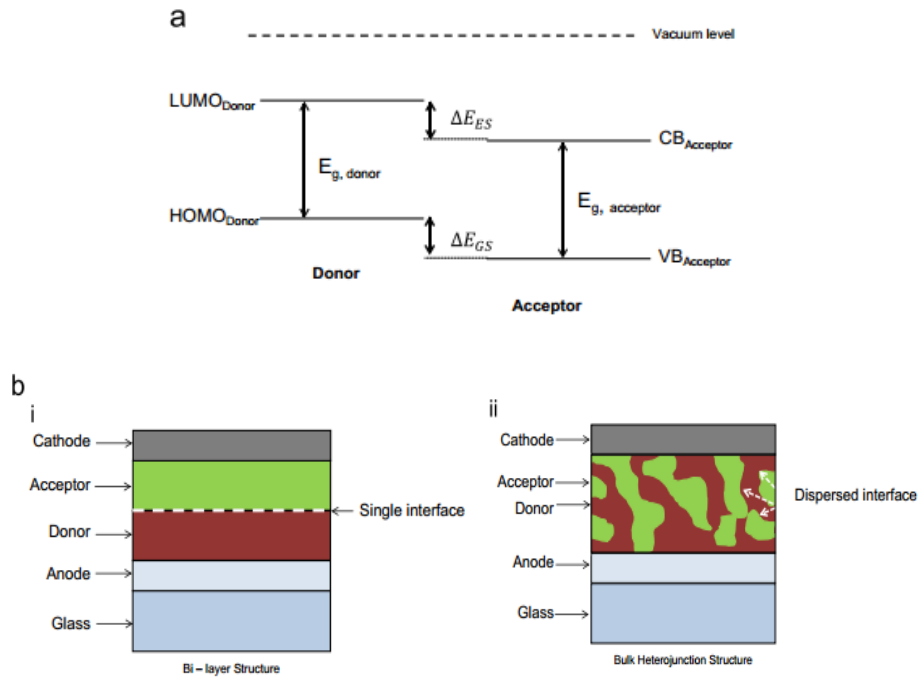

Figure 2-9 (a) Layer heterojunction energy band diagram (b) Schematic of heterojunction (i) photoactive layer (ii) bulk heterojunction PV layer [10]

2.5 Different Layers of Solar Cell:

The solar cell needs four layers to work properly, these layers are of different materials and have their own distinct characteristics and functions. Solar cell efficiencies greatly depend on the correct configuration of these layer, with varying layer material and structure solar cell properties and classification varies. These layers are

- Active layer
- Electron transport layer
- Hole transport layer
- Electrodes

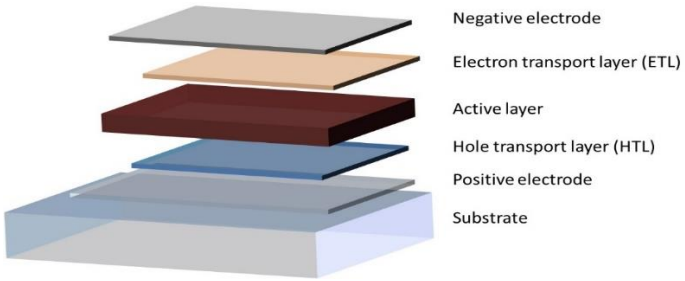

Figure 2-10 Different layers in photovoltaic device

2.5.1 Electron Transport Layer (ETL):

Electron acceptor or electron transport layer which have valance band (VB) values lower than the HOMO of the donor material to efficiently collect the electrons and block the holes to jump.

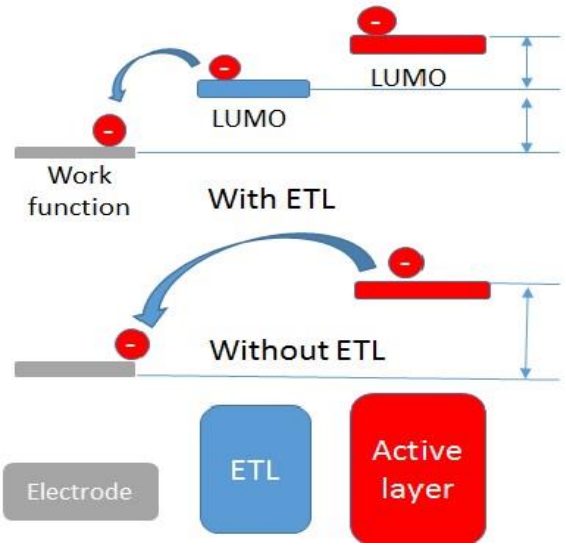

Figure 2-11 Electron to jump in case of ETL and without ETL

Electron transport layer should have optimum Band gap, Charge mobility, Transparency and Chemical stability. CdSe, CdS, CdTe, ZnO, TiO_2, SnO_2, Si, PbSe, and PbS nano-crystals have been used successfully as electrons acceptors.

Table 2-2 PCE of hybrid solar cells with different nano-crystals (NC) and conjugated polymer combinations [9]

NC	Shape	Polymer	PCE(%)	Reference
CdSe	TP	PCPDTBT	3.19	(Dayal et al., 2010)
CdSe	TP	OC_1C_{10}-PPV	2.8	(Sun et al., 2005)
CdSe	QD	PCPDTBT	2.7	(Zhou et al., 2011)
CdSe	NR	P3HT	2.65	(Wu & Zhang, 2010)
CdSe	NR	P3HT	2.6	(Sun & Greenham, 2006)
CdSe	TP	APFO-3	2.4	(Wang et al., 2006)
CdSe	Hyperbranched	P3HT	2.2	(Gur et al., 2007)
CdSe	QD	P3HT	2.0	(Zhou, Riehle et al., 2010)
CdSe	QD	P3HT	1.8	(Olson et al., 2009)
CdSe	NR	P3HT	1.7	(Huynh et al., 2002)
ZnO	-	P3HT	2.0	(Oosterhout et al., 2009)
ZnO	-	P3HT	1.4	(Beek et al., 2004)
CdS	NR	P3HT	2.9	(Liao et al., 2009)
CdTe	NR	MEH-PPV	0.05	(Kumar & Nann, 2004)
CdTe	NR	P3OT	1.06	(Kang et al., 2005)
PbS	QD	MEH-PPV	0.7	(Gunes et al., 2007)
PbSe	QD	P3HT	0.14	(Cui et al., 2006)
Si	QD	P3HT	1.47	(Liu et al., 2010)

2.5.2 Hole Transport Layer (HTL):

It receives the holes from active layer and transport these holes to the anode. Usually PEDOT:PSS is used as HTL in organic photovoltaic cells.

2.5.3 Electrodes:

From the charge transport layer the charges are collected by respective electrodes. The conduction band (LUMO) of electron transport layer, with respect to vacuum level of metal, should be lower than the work function of electrode such that maximum charge collection could occur at cathode. In case of anode its work function should be lower enough from HOMO of HTL to collect maximum holes. Some of the metal used are given in the table with their respective work functions. [10] The electrode with high work function would act as anode and the one with lower work function act as cathode, this difference in work function provides driving force for charges to go to their respective not the other way around.

Table 2-3 Work function of different metals used as electrode

Electrode material	Work function (eV)
Ag	4.5-4.7
Au	4.8-5.1
Al	4.1-4.3
ITO	4.7-5.5
Cu	4.5-5.1

2.5.4 Active Layer:

Active layer is one which receive the photons and convert it into exciton, this exciton then travels in active layer before separation on the donor acceptor interface. This make it most important in modeling power conversion efficiency of final device, its different configuration are introduced due to its morphological importance in which traveling time or exciton diffusion length and separation are perfected. Depending upon different active layer structure three different devices are configured.[9]

2.6 Device Structures in Hybrid Solar Cells:

In hybrid solar cells the three device structure fabricated are,

2.6.1 Bilayer:

Bilayer cells contain two layers of different ionization energies and electron affinity in between the conductive electrodes, the electrostatic force is generated at the interface between the two layers. Materials used for this purpose make differences such large that the strong electric field locally present splits exciton easily enhancing efficiencies in comparison to single layer OPV devices. The layer in OPV which have higher ionization potential and electron affinity is accepted as electron acceptor, and the second layer is donor of electrons. This type of structure in devices is also known as planar donor-acceptor heterojunction. [13]

2.6.2 Bulk Heterojunction:

In these photovoltaic cell a blend of acceptor and donor material is used, this technique has shown promising results in organic photovoltaic. In the bulk form the exciton which has short life span find the interface more likely due to large interfacial area and short diffusion lengths. Organic devices having such structures are easy to fabricate by printing, coating and spray deposition, these could be used for flexible devices.

2.6.3 Comb Structure or Interdigitated:

Morphology is controlled on the nano-scale in such devices which is a difficult task, that's why major issue at such nanoscale is to reduce the recombination possibilities of electron-hole pair. The donor material of thin film has optical absorption length of about 100 nm, while the diffusion length of generated exciton is only 10 nm to 20 nm. Before exciton recombines even if it reaches the D-A interface, the next challenge is to collect the free charges and pass these over to respective electrodes from continuous percolation pathways before charges trap or recombine at interfaces. An interpenetrated donor acceptor comb like structure on the nano-scale would improve the charge transfer, exciton diffusion and charge collection efficiency resulting a higher solar cell efficiency. In Figure 2-9 the heterojunction solar cell is showing a conceptual design of an ideal structure of donor-acceptor phase. [9]

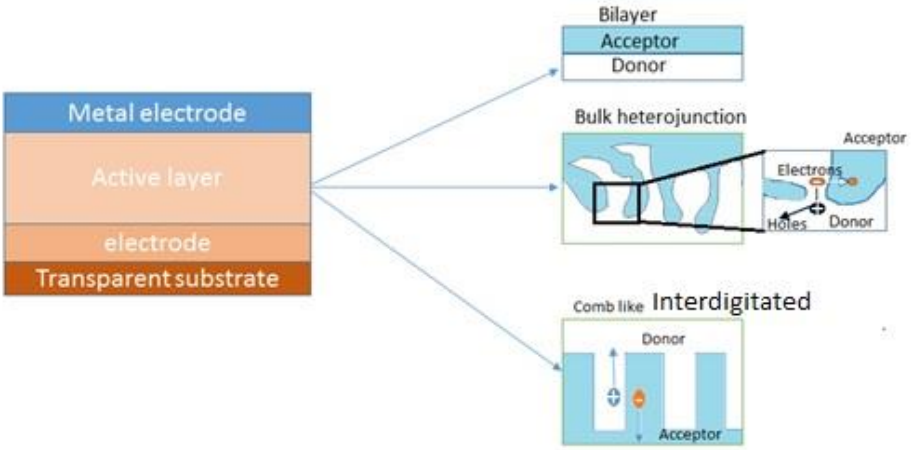

Figure 2-12 Schematic for different device structures for hybrid solar cells [4]

2.7 Terminologies in Photovoltaic:

2.7.1 Power Conversion Efficiency (PCE):

The cost of electricity produced by photovoltaic devices over the years is reduced significantly, as the levelled cost of PV electricity was about 0.5 €/kWh in 2007, which was 0.25 €/kWh at the end of 2011 in Germany. This implies that the cost of electricity should undergo substantial reduction for making a significant contribution to the grid electricity. [14]

One of the approaches made for having cheaper PV electricity is by increasing the power conversion efficiency PCE while keeping PV materials inexpensive. In a solar devices the power conversion efficiency (PCE or η) is given by:

$$\eta = \frac{P_{out}}{P_{in}} = \frac{J_{Sc} \times V_{oc} \times FF}{P_{in}}$$

Where,

V_{oc} = Open circuit voltage

J_{sc} = Short circuit current density

P_{in} =incident input power

FF = Fill factor

For calculating PCE accurately, a standard power source of power input P_{in} with an intensity of 1000 W/m^2 (100 mW/cm^2) is used, with an incident spectrum of Air mass (AM) 1.5 G at room temperature (25^{o}C), these conditions corresponds to clear day sunlight. Under these test conditions, 100 cm^2 surface area of solar cell with 20% PCE would produce 2 W of electricity.

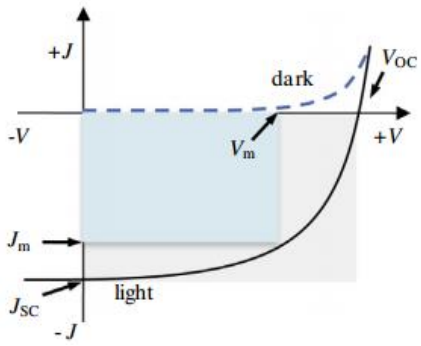

Figure 2-13 Current-Voltage (J-V) characteristics curve for solar cell under illuminated and dark conditions [15]

2.7.2 Factors Effecting PCE:

There are many factors which effects the PCE in photovoltaic device, some of them are

- **Wave length of sun light**: Only photons of specific wavelength range and enough energy are able to generate electron-hole pair, rest generate only heat or reflect back.
- **Band gap**: this is the minimum amount of energy required to free electron from its bond, this energy vary with semiconductors. One reason for low PCE in OPVs is because material band gap doesn't absorb light i.e. 25% of incoming light is wasted. The energy of photons above the band gap is wasted surplus re-emitted as light or heat which accounts for 30% an additional loss. Thus, the inefficient interactions of photons waste about 55% of the incident energy even before exciton generation.[16]
- **Temperature:** Solar cells work best at low temperatures, depending upon materials loses efficiency when temperature raises.
- **Optical losses:** These losses occur when incident light is absorbed by unwanted materials which are not involved in exciton generation.
- **Exciton losses**: Exciton are not able to reach donor-acceptor interfaces due to longer diffusion lengths.
- **Recombination losses**: Electron-hole pair recombination occurs at film defects or at donor-acceptor interfaces.

- **Collection losses:** Charge mobility of transport layer could cause the loss of charge energy before reaching electrode or external circuit.[16]

2.7.3 Internal Quantum Efficiency IQE:

IQE is the ratio of electrons collected by the electrode to the amount of light energy (photons) are absorbed by the solar cell. It is therefore related to external quantum efficiency EQE by the following relation,

$$\eta_{EQE} = \eta_A \times \eta_{EQE}$$

If the thickness of active layer is increased the absorption of incident light also increases but the charge collection at electrodes is significantly reduced. This reduction in charge collection is due to increase in the series resistance Rs which in return cause the decrease in IQE.

For increasing the IQE for a consistent small thickness of thin films an additional layer of metal oxide is used for better charge collection and maximum transfer to the respective electrode. This layer will make sure that electron-hole pair generated by each photon absorbed is collected for maximizing the IQE and in turn increase overall efficiency of the cell.

2.7.4 Air Mass (AM):

AM refers to the standard terrestrial solar spectral irradiance distribution which is quantified as 1.5 in solar cell. [15]

2.7.5 Open Circuit Voltage (V_{oc}):

The voltage provided by an illuminated photovoltaic device when no external load is connected. [15**]**

Important parameter required for working thin film PV device is the open circuit voltage (Voc) which is a built-in potential, it influences charge collection, charge transport and charge dissociation. The voltage across the output terminal is measured when the current is zero, this is open circuit voltage which is given by.[17],[11]

$$V_{oc} = \frac{\mathrm{kT}}{\mathrm{q}} \ln\left(\frac{\mathrm{I_L}}{I_o} + 1\right)$$

Where q stands for electronic charge, k is for Boltzmann's constant, I_L is the current under illuminated condition and I_O is the current dark conditions.

The value of Voc for donor-acceptor bulk heterojunction depends greatly on the difference of energies between the HOMO level of the donor and the LUMO level of the acceptor [17].

$$Voc = \left(\frac{1}{e}\right)\left(|\mathrm{E_{Donor}\ HOMO}| - |\mathrm{E_{Acceptor}\ LUMO}|\right) - \ 0.3\ \mathrm{V}$$

This equation shows that V_{oc} has direct proportional relation to the diagonal band gap, whereas the bulk heterojunction structure is relevant to empirical loss factor here and e is for the elementary charge[11].

2.7.6 Short Circuit Current Isc:

The short circuit current of photovoltaic devices originates from the improved mobility of the charge carriers and from enhanced interfacial contacts between the donor and the acceptor [17].

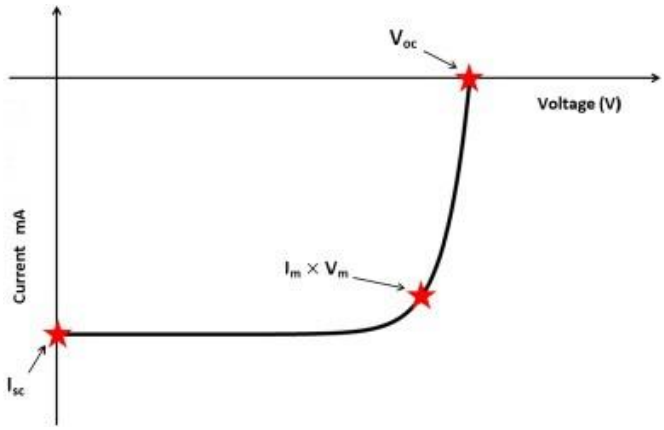

Figure 2-14 Current and Voltage (I-V) characteristics curve of illuminated solar cell

The short circuit current Isc divided by the area of solar cell give us the short circuit current density (Jsc), at short circuit conditions it is the maximum photocurrent density which can be extracted from the device. It could be expressed as

$$J_{SC} = qG\left(L_n + L_p\right)$$

Where G is the parameter for charge generated while Ln and Lp represents the hole and electron diffusion lengths respectively.

The current density is in direct relation with the external quantum efficiency (*EQE*). The EQE is the ratio of collected photo generated electrons to the number of specific wavelength photons incident at device. The relationship of Jsc and EQE can be given by:

$$Jsc = \frac{q}{hc}\int_{\lambda min}^{\lambda max} EQE \times Pin\,(\lambda)\lambda \times d\lambda$$

For hybrid solar cell to operate, the EQE is dependent on five unique efficiencies. Therefore EQE can be formulated as:

$$EQE = \eta_{abs} \times \eta_{diff} \times \eta_{diss} \times \eta_{tr} \times \eta_{cc}$$

Where,

η_{abs} = Absorption efficiency

η_{diff} = Exciton diffusion efficiency

η_{diss} = Exciton dissociation yield

η_{tr} = Efficiency of charge carrier transport throughout device

η_{cc} = Efficiency of charge collection at the electrodes

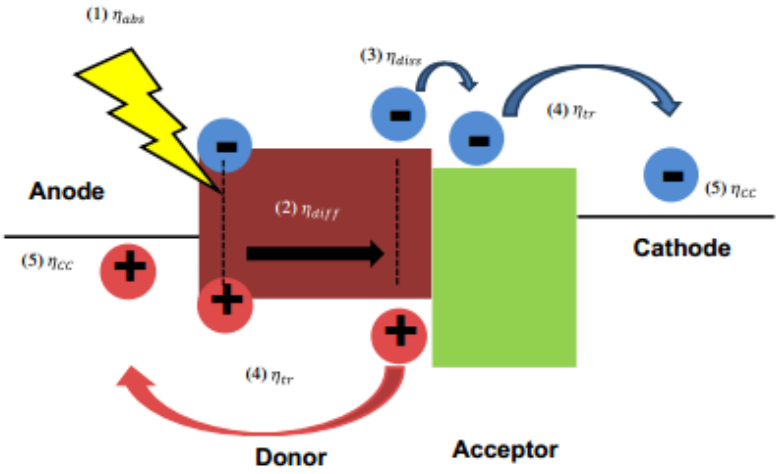

Figure 2-15 Key step in charge transfer process [10]

The figure 2-12 is illustrating the five key steps in process of charge transfer and the corresponding efficiencies in the energy band diagram. The external quantum efficiency EQE is the combined effect of these efficiencies. [10]

2.7.7 Fill Factor:

Fill factor is the ratio of the actual power to maximum power a solar cell can. Maximum predicted power is the product of short-circuit current Isc and open-circuit voltage Voc, while

the actual maximum power is product of Im and Vm [17]. Fill factor is described as the 'squareness' of the *J–V* curve shown in Fig 2-10. It is defined as:

$$FillFactor = \frac{Im \times Vm}{Isc \times Voc}$$

Where,

Jm = maximum power point current density

Vm = maximum power point voltage

The ideal value for FF is 1 but experimental value is always less than 1 because of physical constraints of material quality and other internal losses. Organic thin film photovoltaics with fill factor of 0.65 are reported. The behaviour of an experimental diode will deviate from ideal fill factor value, because of recombination of electron hole pairs at donor-acceptor interface in heterojunction solar cells. [10]

2.7.8 Factors Effecting Fill Factor:

2.7.8.1 Parasitic Resistance:

Parasitic resistance includes the series and shunt resistance, whose effect could lower the FF of the device. Figure 2-13 shows shunt and series resistance in solar cell.

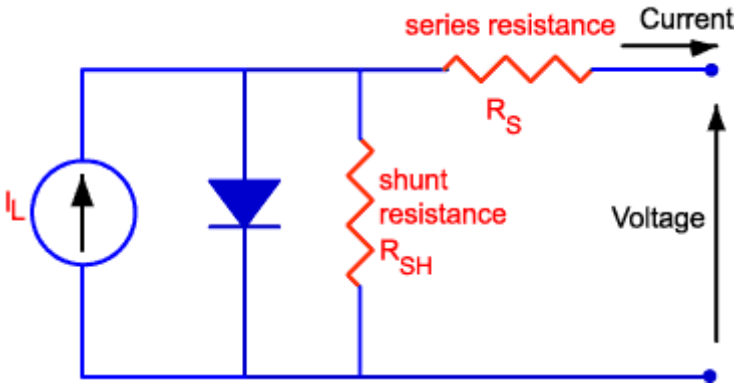

Figure 2-16 Series and shunt resistance in solar device [18]

The impact and magnitude of both resistance depends upon the operating point and geometry of solar device. The value of the resistance depends upon the area of solar cell for this purpose current I is converted to current density J, giving the resistance units as Ωcm^{-2}.

$$R = \frac{V}{J}$$

Where,

R = Parasitic resistance

High series resistance effects the V_{oc}, the resistance is because of metal contacts while shunt resistance reduces the current by providing alternating path for charge. [18]

2.7.8.2 Recombination:

Electrons are excited when absorb the incident photons, but due to different reasons like defects, diffusion length, interface the electron in exciton now in conduction band stabilize itself to valance band releasing hole and energy. This is called recombination.

2.8 Problem Statement:

For understanding the problem, we have to consider the an inverted hybrid solar cell model and focus on the moving electrons in it as illustrated in figure 2-14 . When the light is absorbed by the active layer in device an electron-hole pair (exciton) is generated, this generated electron have some major problems here to worry about before getting out in to external circuit, one is to find the interface at shortest distance which is related to active layer.

Once it finds the interface now comes the second hurdle that is to dissociate at interface and give away the electron to electron acceptor. Here it mainly depends upon electronic properties of electron transport layer, the energy levels LUMO and band gap which effects the dissociation. If the necessary force is not provided by electron transport layer for the dissociation the electron-hole pair recombines and thus decreasing overall performance.[19]

The electrons that successfully jumps to the electron transport layer are now depending on its charge mobility and its relation of energy level with electrode ITO coated glass in this case.

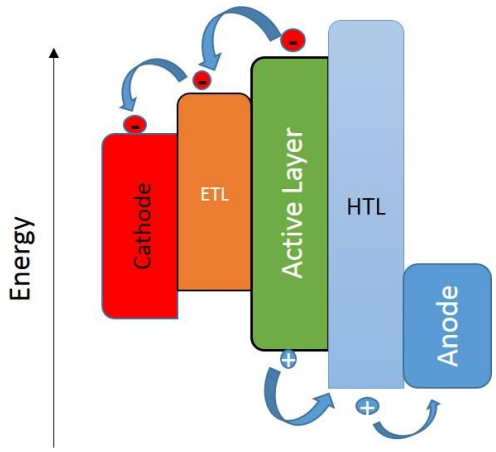

Figure 2-17 Schematic of charge transfer in solar cell

2.9 Purposed Solutions:

For the problem of charge dissociation at interface many metal oxide are used as electron acceptors for increase charge collection. Metal oxides like TiO_2, ZnO, CdS, CdSe etc. ,each of these are used as electron transport layer and have unique properties of its own, TiO_2 has been used often due to good PCE but has lower electron mobility, an alternate for this is ZnO which has much better electron mobility but has lower PEC due to its surface morphology. As we are focusing on band gap studies ZnO is more viable for this research. As the energy level LUMO of the ETL acceptor must be matching the work function low enough of cathode.

And the other issue regarding the band gap reduction for better charge transport to the ITO, for this purpose 2 dimensional materials are showing great promises as graphene is used before due to zero band gap which help in reduction in band gap. Here we are purposing exfoliated monolayer MoS_2 as it has also low direct band gap of 1.2-1.3 eV, which will hopefully help in reduction of ETL band gap. This will shift the band gap from ultra violet region to visible region.

Chapter 3

Materials for Photovoltaic devices

3.1 Active Layer Materials:

In comparison to a double-layer configuration of active layer, the advantage of a bulk heterojunction is enormously enhanced thicker photoactive layer and interface area, optimized for light absorption, which can be easily implemented in the solar device. The challenge is to choose and arrange the optimum materials in active layer i.e. donor and acceptor both, such that we get maximum interfacial area. This optimization will ultimately decrease the diffusion length and provide a continuous and short path for charge carriers transportation to respective electrode.[20]

3.1.1 Donor Materials:

Electronic properties and hole mobility are important while selecting suitable donor material. Donor materials are selected relative to acceptor material. HOMO and LUMO levels and band gap are of particular significance in selection. Scharber et al. suggested that by following designed guidelines while choosing donor material to be used along PCBM acceptor for an organic device could give PCE above 10%.[10] It has been also suggested that for greater PCE values the band gap range should be less than 1.74 eV and LUMO should be less than 3.92 eV, based on vacuum level[16].

Large amount of solar energy can be utilized by using small band gap materials and still maintaining the large enough offset level of LUMO to facilitate exciton dissociation. A donor material Phenylene vinylene (PPV) with relatively low PCE due to low hole mobility was used before it was replaced by more beneficial and preferred donor material which is a polymer, this material with enhanced properties is P3HT (Poly 3-hexylthio-phene). P3HT has superior properties like environmental stability, higher absorption and hole mobility. The possible band gap and current density for various polymers of low band gap used as electron donor are given in table 2-4.[20] Different polymeric materials including silicon are given along with there band gap, wavelength and current density Jsc, the material with lowest possible band gap have maximum Jsc and wavelength which is also higher than P3HT. PTB7 has excellent hole mobility, solubility in organic solvents, charge transport favourite position and good photovoltaic capabilities.[21]

Table 3-1 Properties of donor materials [21]

Materials	Band gap (eV)	Wavelength (nm)	Current density (mA/cm^2)
P3HT	1.85	672	19.756
PTB7	1.74	714	22.818
PCPDTBT	1.4	887	34.288
Silicon	1.12	1109	45.167

The polymer material selected must be a less HOMO energy level to give a large Voc and optimum LUMO energy level to give offset enough for charge dissociation. [21]

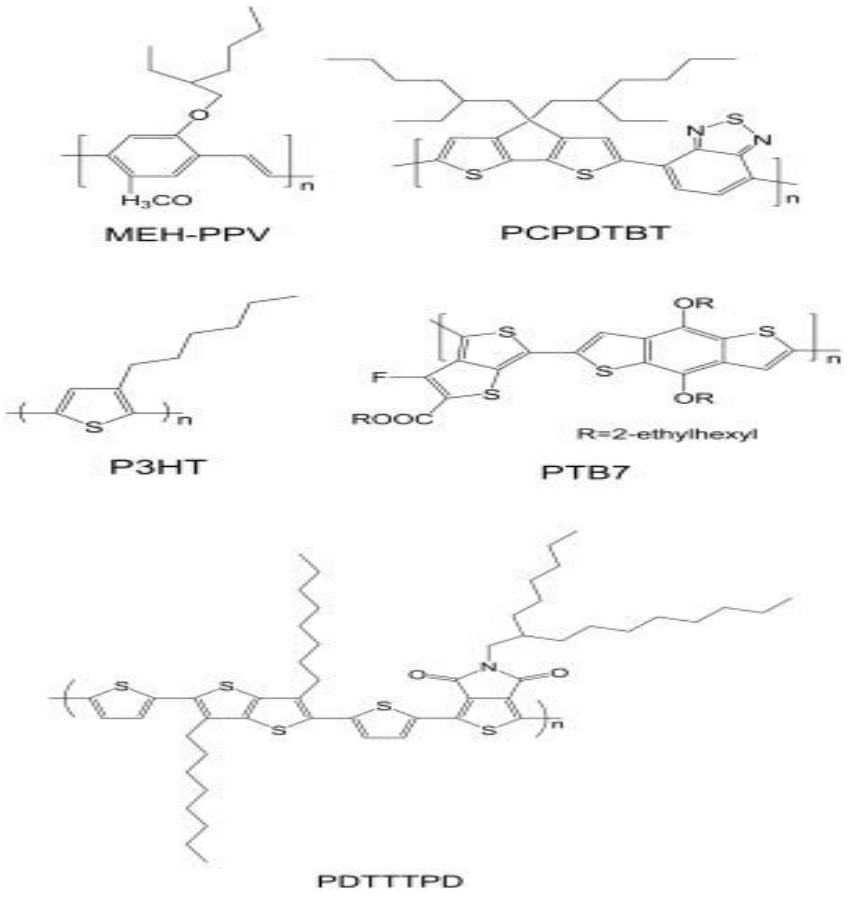

Figure 3-1 Chemical structures of donor materials used in OPV [20]

3.1.2 Acceptor Material:

Fullerenes when used along with P3HT give some benefits, one of many is its good solubility but along this there are few limitations like environmental stability and limited absorption contribution. These issues could be overcome by using an inorganic materials instead of fullerenes. Major advantages are of modifying physical dimension of nanoparticle for tuning the band gap of inorganic semiconductor.[22]

P3HT, PPV and PCBM are organic polymer undergone several strict analysis for the purpose of optimization. The factors like weight percent ratio of acceptor and donor, there solvents, maximum light trapping and annealing temperatures and rate for different improved nano-morphology having good degree of crystallinity to facilitate maximum charge transport to respective electrode are optimized.as shown in fig. 3-2.

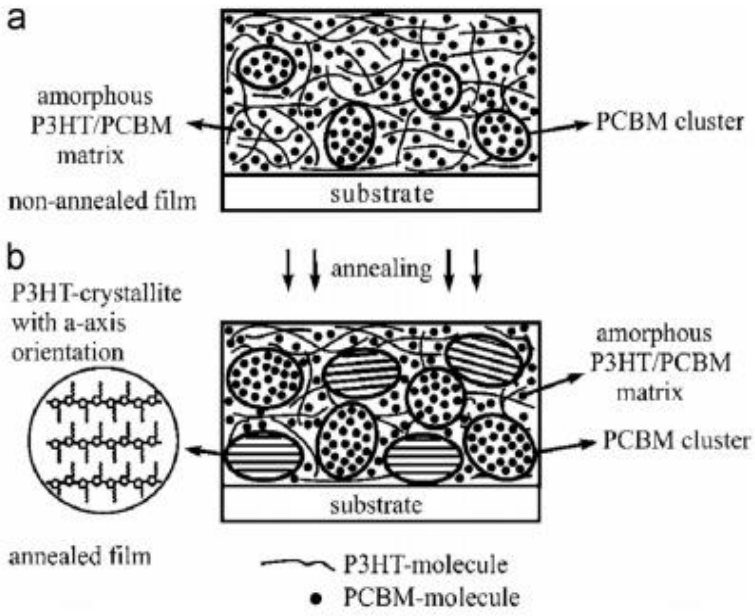

Figure 3-2 Schematic for P3HT: PCBM blend film, morphology changed due to annealing.[23]

Fig 3-2 is illustrating the difference between micro structures of P3HT/PCBM matrix thin film one annealed and other is not. The amorphous structures can be seen and after annealing these structure more crystalline an arranged structure which has enhanced electrical properties.

The crystallite structure of thin film matrix is more oriented. UV-vis spectroscopy is used to classify the effect of annealing thin films over absorption profile. Thermal annealing have

noticeable effect on two major phenomena, one is the red shift of absorption peak and absorption magnitude is increased for P3HT:PCBM blend.

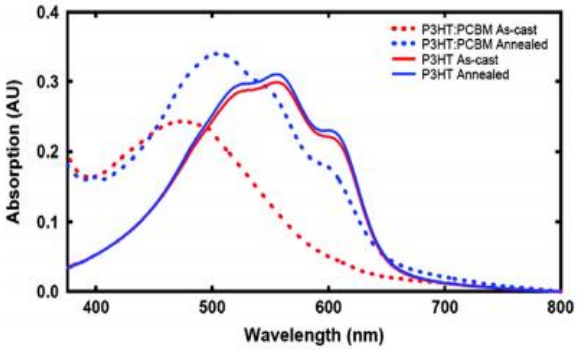

Figure 3-3 UV–Vis spectrum of thin films annealed and non annealed of P3HT and P3HT: PCBM[10]

The material's band gap should be minimised to have good photon absorption and high *Jsc*, and also to utilize the maximum of incident solar spectrum. The Voc of the material can be maximised by using high conduction band acceptor material, as *Voc* dependents greatly on the heterojunction with diagonal band gap.

Another electronic requirement for the inorganic acceptor material in accordance with donor is material ground state offset, when acceptor material absorbs light for exciton dissociation it is required.[10]

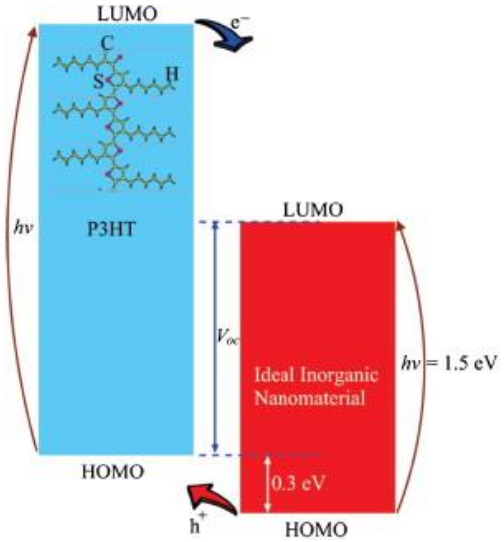

Figure 3-4 Schematic diagram showing P3HT coupled to inorganic material in ideal electronic configuration [10]

In Figure 3-4, the band gap of inorganic material is 1.5 eV, which represents balance between energy offset and absorption for high *Voc*. For maximum Voc, the offset of 0.3 eV at HOMO level is enough to overcome the electron-hole pair binding energy.

3.2 Materials Currently Used:

An electronic heterojunction with interface between two semiconductors is designed, this design have different characteristics like electron affinity, band gap and ionization potential. A common combination for heterojunction may result in working photovoltaic device but the system efficiency is greatly dependent on materials ionization energy, band gap, electron appreciation and solubility in organic solvents.

Different component system are used for manufacturing the PV device, some of materials which are often used as acceptor and donor are mentioned along with their HOMO,LUMO levels and band gap in Figure 2-18. Some of important electron acceptor materials are ZnS, TiO_2, ZnO, PbS, Si, CdS, CdTe and CdSe, each one of these have individual electronic characteristics.

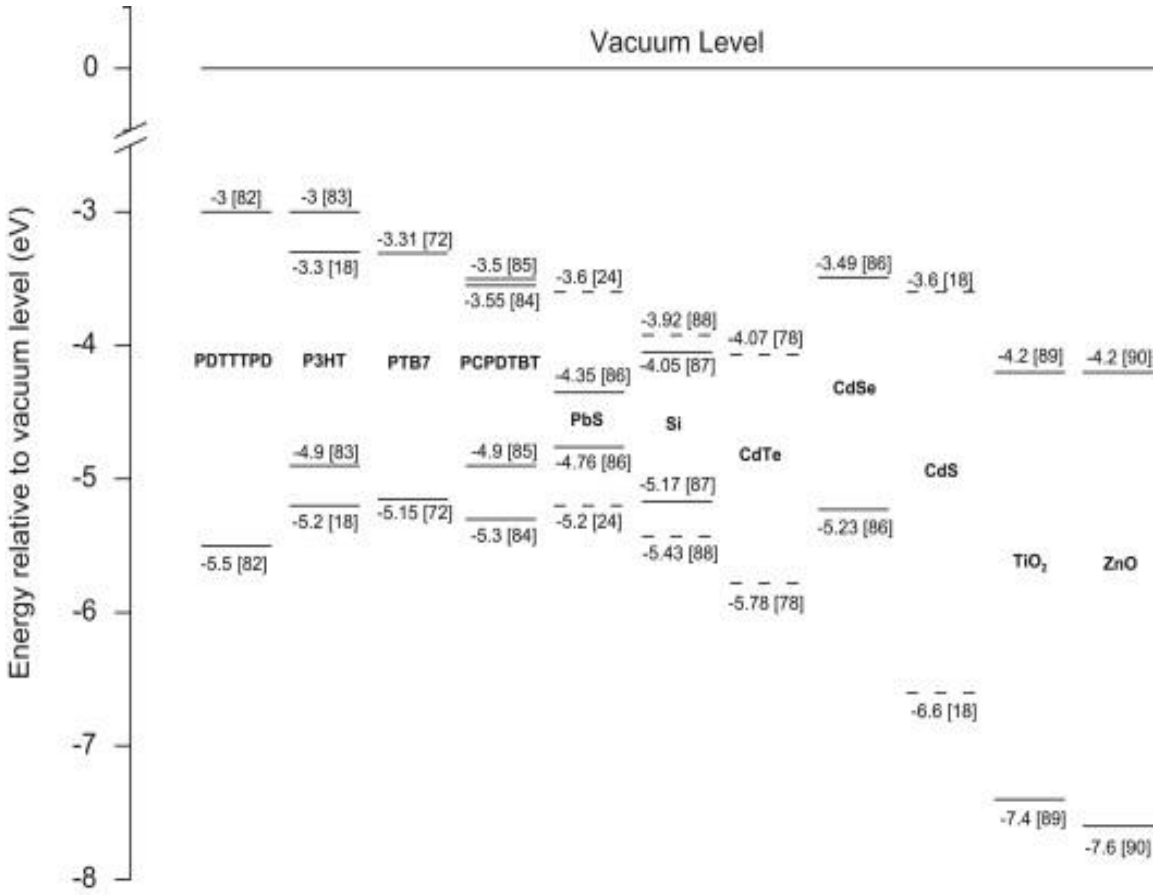

Figure 3-5 Energy band gap of different donor and acceptor materials used in OPV. [10]

3.3 Metal Oxide Nanoparticles:

Wide band gap oxide semiconductors have also been investigated as inorganic acceptors in several hybrid solar cells. Elements which have been analysed involve TiO_2, SnO_2, CeO_2, and ZnO. The important advantage of these semiconductors is the ability to form vertically aligned oxide nanostructures for the optimization of a large D–A interfacial area, as well as providing effective conduction pathways.[24],[25] This gives a large dissociation and reduced electron hopping steps, thus enhancing electron mobility.

3.4 Zinc Oxide (ZnO):

ZnO thin films have shown great interest as transparent conductor, due to their promising properties. ZnO is an n-type wide band gap semiconductor (Eg = 3.34 eV).Zinc excess at the interstitial position make it electrically conductive. Over the decades the electrical properties are modified by thermal treatment with hydrogen/air environment or by doping process.[26]

3.4.1 Properties of ZnO:

Zinc Oxide (ZnO) is unique as it exhibits both semiconducting and piezoelectric properties. ZnO is a material having diverse structures, its configurations are much more than any other known nanomaterial including carbon nanotubes.[27] ZnO has also received considerable attention as a promising material for solar cell applications due to its nontoxicity, good stability, good electrical and optical properties, and low cost.[26]

3.4.2 Physical Properties:

ZnO has a stable wurtzite structure with a=0.325 nm and c=0.521 nm. The wurtzite structure (Figure 3-6) has an ABAB hexagonal close packing (HCP) structure. The structure of ZnO consists of alternating planes composed of O^{2-} and Zn^{2+} ions which are tetrahedrally coordinated and stacked along the c-axis on an alternate basis (Figure 3-6). The Zn^{2+} and O^{2-} ions create a normal dipole moment and instant polarization which results in a diversification of surface energy.

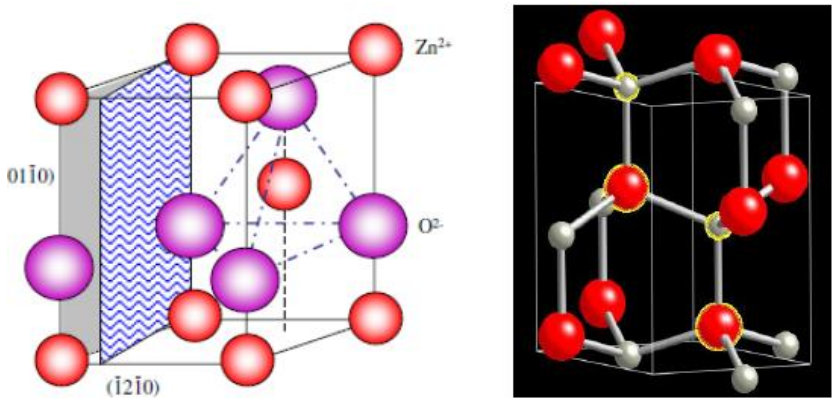

Figure 3-6 Wurtzite structure of ZnO

3.4.3 Electrical Properties:

Zinc oxide-ZnO has a wide direct band gap of 3.37eV and large exciton binding energy of 60 meV. Along with these electrical properties, ZnO has the potential application in different fields as in chemical sensors, solar cells, luminescence devices etc. ZnO nanowires reported also have behaviour like n-type semiconductor due to the presence of interstitial defects and vacancies. ZnO is transparent to visible light and doping can made it highly conductive.[28]

3.4.4 Optical Properties:

The main focus of studies right now is the intrinsic optical properties of ZnO nanostructures as they can be used for implementing photonic devices, photoluminescence (PL) spectra of ZnO nanostructures have been widely reported. Exciton emissions have been observed from the PL spectra of ZnO nanorods. It is reported that exciton binding energy can be greatly enhanced if we confine the quantum size but an interesting observation is that the green emission intensity increases with a decrease in the diameter of the nanowires. This is due to the larger surface-to-volume ratio of thinner nanowires which favours higher level of defects and surface recombination. Some application include optical fibres, surface acoustic wave devices, solar cells etc. [28]

3.4.5 ZnO Structure:

Nano-sized zinc oxide have great variety of nano structures which means zinc oxide can be placed among materials with new potential applications in various fields of nano-technology. ZnO can occur in 1D, 2D and three-dimensional (3D) structures. 1D structures includes nano-

rods, needles, ribbons, helixes, springs and rings, combs, wires, belts and tubes. Zinc oxide obtained 2D structures are, nano-pellets and nano-sheet. 3D structures of zinc oxide can be obtained as flower, snowflakes, dandelion like, etc. Different examples of ZnO nano structures are given in Figure 3-7. These different structures can be obtained by varying the synthesis techniques and reaction parameters.

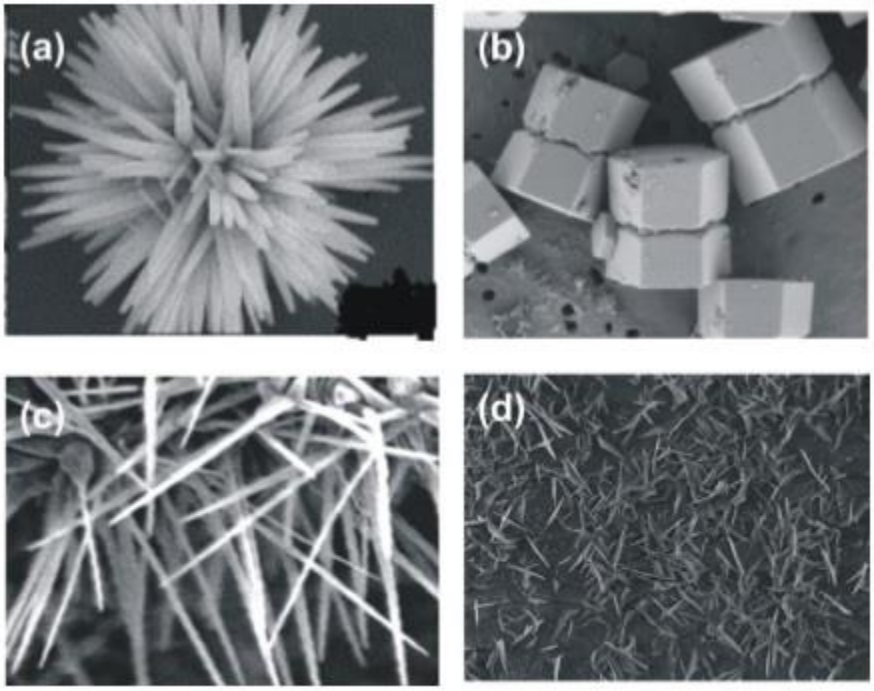

Figure 3-7 Scanning electron Microscope (SEM) of ZnO structures a) flowers b) nano rods (c,d) nano wires [27]

3.5 Transition Metal Dichalcogenides (TMDs):

TMDs have general formula MX_2 where M belongs to earth transition metals from group IV, V, VI and X represents the chalcogenide (Se, S or Te) from group XVII of periodic table. TMDs have strong intra plane covalent bonding and week inter plane Van der Waal forces, which make it easy to separate its layers by exfoliation and less harming the in plane bonds to get sheets. TMDs like MoS_2, MoSe, WSe_2 and WS_2 have large applications in fields of photovoltaic, transistors and electro-luminescent because of the sizeable band gap. TMDs have hexagonal or rhombohedral and the metal atoms have octahedral or trigonal prismatic arrangements.[29]

By the discovery of 2D layered materials, TMDs scope has also been widely broaden due to the super properties of electrical and thermal conductivities, band gap and charge mobility like Graphene.[29]

3.6 Molybdenum Disulphide MoS_2:

Molybdenum disulphide (MoS_2) belongs to the group VI family of transition metal dichalcogenides (TMDs).It is an indirect band gap semiconductor. The crystalline structure of MoS_2 consists of stacked S−Mo−S sheets which gives it various physicochemical properties such as solid lubricants and catalysts, also crystals of MoS_2 along with other semiconducting TMDs such as $MoSe_2$ and WSe_2, could be used as stable photo electrochemical electrodes and photoactive material. Subsequent study on polycrystalline MoS_2 thin films showed a photoelectric response comparable to single crystals. More recent, methods for producing thinner sheets have been explored with larger yields via intercalation, exfoliation and chemical means.[30],[31]

3.6.1 Structure:

The bulk MoS_2 crystal is built up of van-der-Waals bonded S-Mo-S units. Each of these stable units consists of two hexagonal planes of S atoms and an intermediate hexagonal plane of Mo atoms, having coordinated covalent interactions with the S atoms in a trigonal prism like arrangement (Fig. 3-8). Because of the strong interlayer interactions and relatively weak interactions between these layers, the formation of ultrathin crystals of MoS_2 by exfoliation is possible.[31]

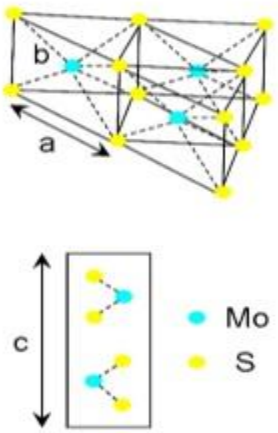

Figure 3-8 MoS_2 atomic arrangement in bulk [32]

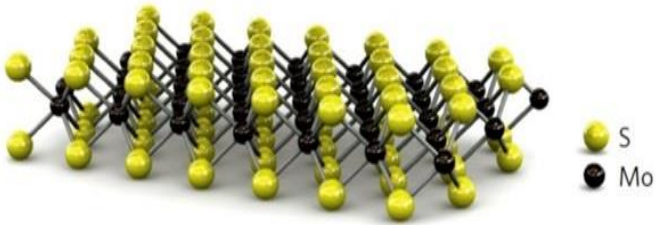

Figure 3-9 MoS_2 mono layer arrangement [32]

3.6.2 Optical and Electrical Properties:

The two dimensional nano sheets offer unique optical and electrical properties as compared to bulk MoS_2.

Photoluminescence in MoS_2 with its decreasing layer thickness surprisingly increases. Probably due to quantum confinement in d-electron layered materials, the photoluminescence is strongest in monolayer and this could also explain the crossover of indirect band gap to direct band gap from bulk to monolayers.[33]

Higher sunlight absorption of monolayer TMD than the currently used materials make MoS_2 appealing for photovoltaic devices. And higher charge mobility of 200 $cm^2/V.s$ in monolayers are coupled to ultrathin solar devices or monolayer PV devices with low series resistance, high charge mobility, large voltages and optimum I-V curve.[34]

Transparency of monolayer MoS_2 is also very high Like other 2D materials such as graphene which about 97% transparent. This property make it important material for its use in optoelectronics along its other super electrical and conductive properties.

Indirect Band gap of MoS_2 in bulk form is 1.2-1.3 eV and also direct band gap of 1.29eV. When MoS_2 bulk is reduced to monolayers the indirect band gap increases to 1.70ev but the direct band gap remains at 1.30eV with very little change of 0.1eV.[32]

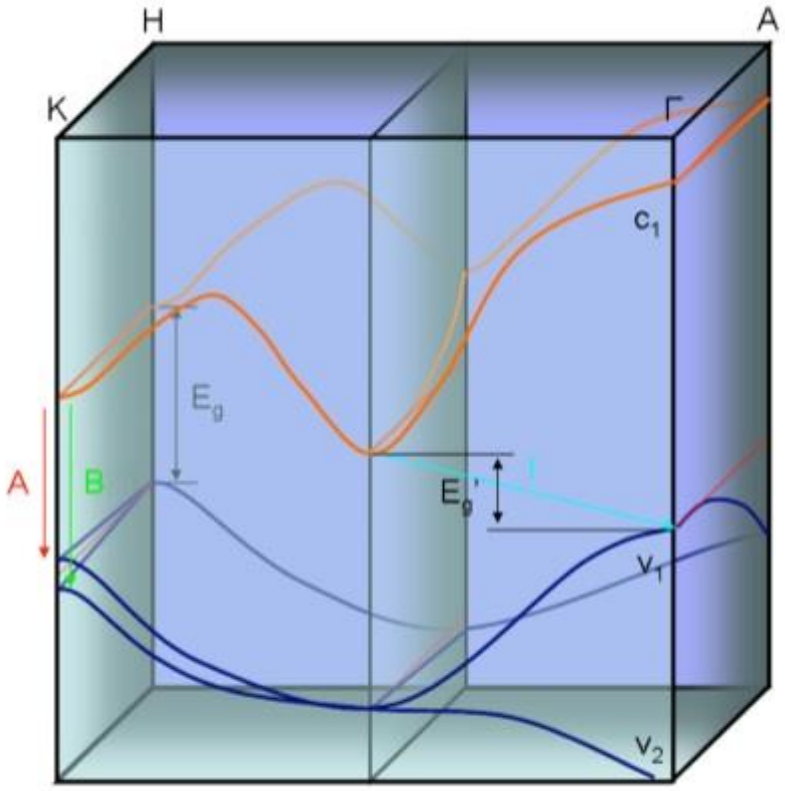

Figure 3-10 MoS_2 direct Eg and indirect band gap Eg' [32]

In Figure 4.- transition A to B shows the direct band gap transition from bulk MoS_2 to monolayer. And I is indirect band gap. Eg and Eg' are the direct and indirect band gap of bulk MoS_2 respectively. This clearly explains that there is very little difference in A and B the direct band gap, while the diagonal increase in I from V1 to V2 is pretty large. For monolayer the indirect band gap crossover to direct one, therefore only direct band gap is considered in studies.[32]

Chapter 4

Synthesis route and Characterization Techniques

4.1 Molybdenum Disulphide (MoS_2) Exfoliation:

TMD are becoming favorite materials for next generation electronics because of the exceptional electrical, thermal and charge carrier properties. Many techniques have been used to get thin sheets of MoS_2 like Liquid Phase Exfoliation, micro exfoliation (mechanical), chemical process and electrochemical process. Liquid phase exfoliation is most preferable because of simplicity, reproducibility and economical.[18]

4.1.1 Liquid Phase Exfoliation:

For this technique MoS_2 powder is added to a solvent mostly used is NMP as 1mg/5 ml. The setup should be set carefully by placing a probe sonicater into the solvent without touching beaker walls and left for continuous sonication for 66 hrs. The system was placed in the chiller at 2^oC to keep the solvent cooled and remove heat generated by sonication. Higher temperatures could lead to solvent evaporation and re-coagulation of exfoliated sheets. Some important parameters to be considered due sonication are the solvent concentration, sonication time and temperature.

After successful sonication the suspension is removed and centrifuged at 4000 rpm to get fine sheets. The supernatant was filtered using 0.22 micron nylon filter, after drying MoS2 was dispersed in the desire solvent and concentration by mild bath sonication.[30]

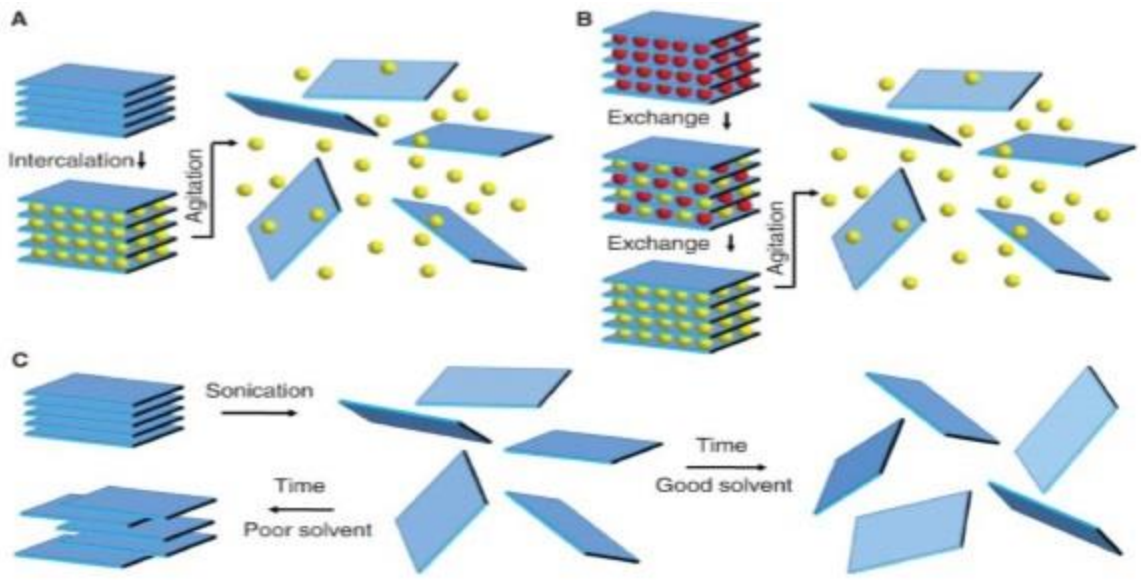

Figure 4-1 Exfoliation due to continuous sonication to overcome week secondary forces and solvent dependency[18]

4.2 ZnO Synthesis:

Many synthesis routes for ZnO are reported in literature like

- Mechno-chemical process
- Precipitation process
- Sol gel
- Solvo-thermal
- Hydrothermal techniques.

All these technique leads to ZnO but with varying nano structures like rods, flowers, wire etc. [35, 36]

4.2.1 Sol Gel:

This technique is very useful in getting ZnO nano powder and thin films and is also used excessively due to its simplicity, repeatability, low cost and mild processing conditions, which also enable ZnO surface modification by different organic compounds. This modification of ZnO leads to different properties and applications. Synthesis of ZnO via sol gel gives nanoparticles which are used in optoelectronics applications.[35],[36]

Figure shows different routes which could be adopted by using sol gel synthesis technique. Route (a) leads to thin film from the colloidal sol which have extensive use in photovoltaic devices while (b) leads to nano powder ZnO when sol transforms to gel and then dried.

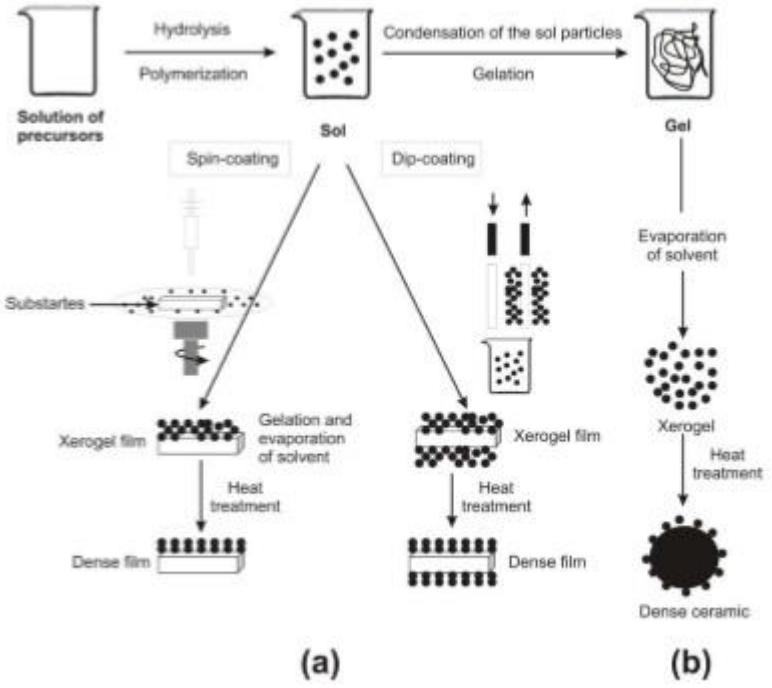

Figure 4-2 Sol gel Synthesis route for a) thin films b) gel and nano powder[37]

4.2.2 Spin Coating

To obtained thin films coated over a substrate usually glass spin coating technique is used. Spin coating gives a smooth and uniform thickness film. And the instrument used for this purpose in this study is "SCS G-8 Spincoat". Different variables like spin time, acceleration time, spin speed are available to control film thickness. Spin speed is used to vary film thickness, higher the spin speed and time the thinner are the coated films. A vacuum pump is part of spin coat assembly, its purpose is to hold the substrate while spinning. It uses the natural phenomenon of centrifugal force to spread film while spinning. And factors effecting it are viscous forces, centrifugal force, solution substrate adhesion, surface tension, concentration of suspension and evaporation rate of solvent. Uniform film coating requires the solvent of low viscosity and non-volatile at high spin speeds. The film coated are usually amorphous which are annealed at high temperatures to achieve crystallinity. [37]

Figure 4-3 SCS G-8 Spincoat

4.3 Characterization Techniques:

4.3.1 Scanning Electron Microscope (SEM):

In this era of nano technology scientist must be able to study, analyse and characterize the materials at µm and nm (nano-meter) scale for successful results. For the purpose of observation and microstructural characterization Scanning electron microscope is a power helping tool. In this technique area under observation is examined by irradiating the focused area by electron beam which interacts with specimen surface and near surface area. The interaction of electron beam with the specimen may vary, generating different signals. Different signal received by unique detectors are Secondary electrons SE, Back Scattered electrons BSE, characteristic X-rays, Auger electrons and varying energy photons. Each signal gives different characterises of the specimen like surface topography, composition and crystallography.

SE and BSE signals are of importance because they are generated at or near surface when electron beam scan, giving great surface topography images. On electron beam bombardment characteristics X-rays are generated which gives qualitative and quantitative analysis by composition mapping.

Some of important features are SEM's three dimensional imaging of specimen appearance, direct field depth results and shadow relief effect.

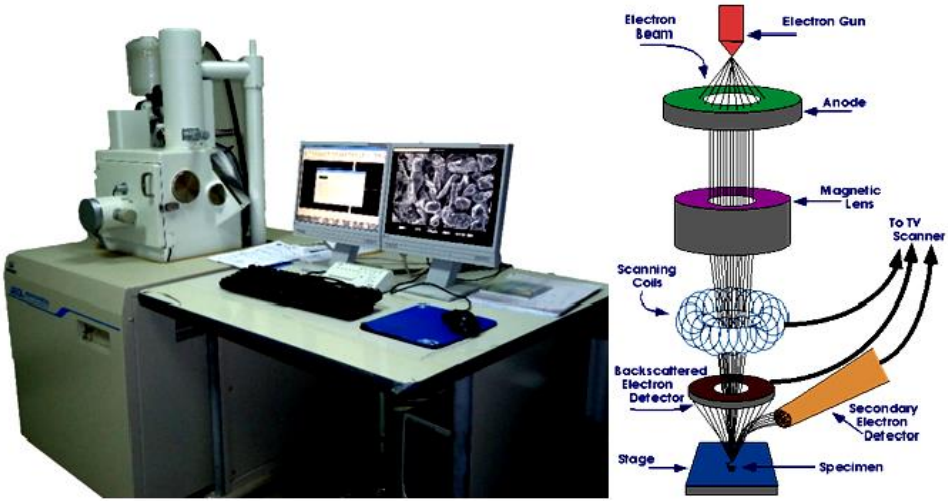

Figure 4-4 Scanning Electron Microscopy a) JSM 6490 LA in SCME b) SEM schematic

4.3.2 Atomic Force Microscopy (AFM):

AFM or SPM (scanning probe microscope) is the technique used for imaging topography and surface properties such as roughness, and mechanical properties. Very sharp tip (few atoms thick) attached to the edge of cantilever is raster scanning the specimen, the tunnelling current between tip and sample is kept constant, tip changes its position to keep distance constant. Laser reflected from the cantilever falls on the four quadrant photo sensitive diode (PSD) which uses the tip deflection as function of position to create a surface image. Image from AFM is not real image.

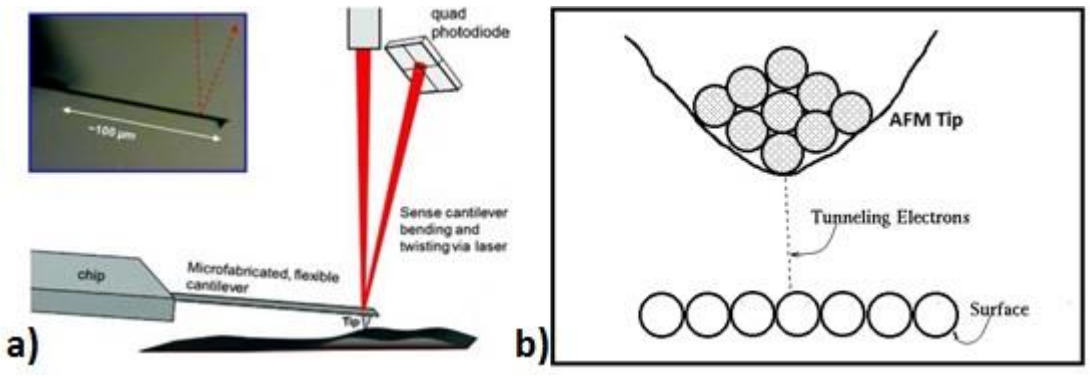

Figure 4-5 AFM a) schematic diagram B) Interaction between tip and surface

Van dar Waals force between tip and sample play an important in AFM as the tip raster the specimen tip move up and down because of attraction and repulsion by Van Dar Waals force.[38] This tip movement is recorded by PSD as mentioned in Figure 4.5

Different uses of AFM are its ease of use, easy sample preparation, repeatability and accurate height of specimen. Some of the ways of using AFM are imaging topography, surface modification, measuring properties and sensing device.[38]

Figure 4-6 JEOL (JSPM-5200) Atomic Force Microscopy (AFM)

4.3.3 X-Ray Diffraction (XRD):

XRD is the technique used to determine the lattice parameter and crystal structure of the sample. Generally x rays of predefined wavelength are incident onto rotating sample at particular angles, the rays are diffracted by the atoms in the sample. Some of x rays diffracted are in phase and some of these are out of phase, forming the constructive and destructive interfaces respectively. These diffraction greatly depend upon the distance between different planes in material parallel to each other, these distances vary with varying elements and compounds.

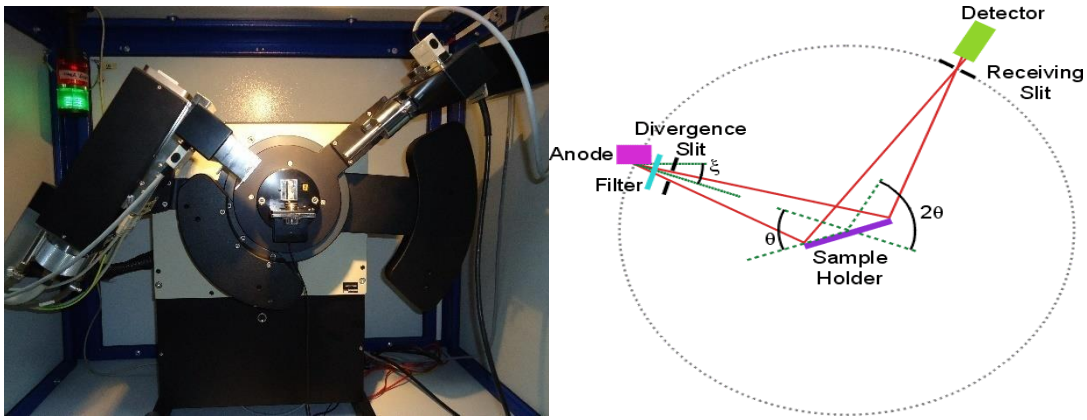

Figure 4-7 a) X-ray Diffraction Machine XRD model STOE $\boldsymbol{\theta - \theta}$ b) Schematic of XRD

The single generated by the in phase x-rays after reflection from material are collected by the detectors and are compared to x rays before reflection. The results are quantifiably represented by using Braggs Law,

$$n\lambda = 2\mathrm{d}\sin\theta$$

Where n is order of diffraction, d is the spacing of planes, λ is the wavelength and θ is the angle of reflection. Wavelengths only for which Bragg's reflection happens are $n\lambda \leq 2\mathrm{d}$, this is the reason visible light couldn't be used as no diffraction will occur. And the diffractions can only happen on the specific angles for particular lattice planes as predicted by Bragg's Law.2θ angle used for ZnO-MoS_2 films is in range 5-50 and the step size was 0.04.

4.3.4 Electrochemical Spectroscopy/ Cyclic Voltammetry (CV):

Electrochemical spectroscopy is recent technique in electro-analytical chemistry replacing old polarography. CV not only limits its applications to measuring thermodynamically oxidation reduction process but also provides the kinetics of chemical reactions and electron transfer reactions. The unequivocal position of voltammetric waves as result of electrochemical redox process give CV the name 'Electrochemical spectroscopy.[39]

In our case we are using CV to calculate the HOMO (highest occupied molecular orbit) and LUMO (Lowest unoccupied molecular orbit) of our charge transport layer and band gap is calculated from there. This information is important in grouping of donor and acceptor in accordance with levels calculated, for photovoltaic devices. The onset of oxidation and reduction curves from CV are calculated and used in below equations for HOMO and LUMO values.

$$E_{HOMO} = E_{onset}^{oxd} - 4.8$$

$$E_{LUMO} = E_{onset}^{red} - 4.8$$

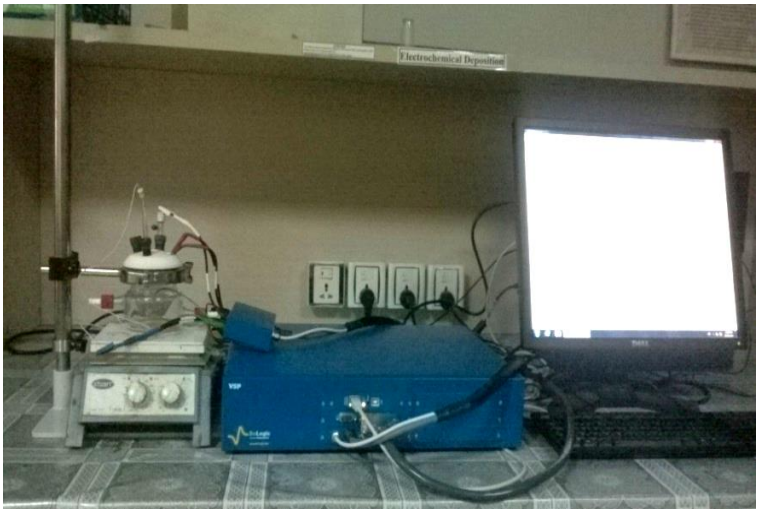

Figure 4-8 Cyclic Voltammetry or Electrochemical Spectroscopy

4.3.5 UV-VIS Spectroscopy:

UV-VIS spectroscopy is used to measure spectrum of the specimen, spectrum is the graph between the intensity of transmitted or absorbed radiations vs the wavelength or frequency. UV range is 180-400nm and visible region is 350-800nm when photons of this wavelength are bombarded onto sample some of them are absorbed and other transmitted leaving very little to be reflected.

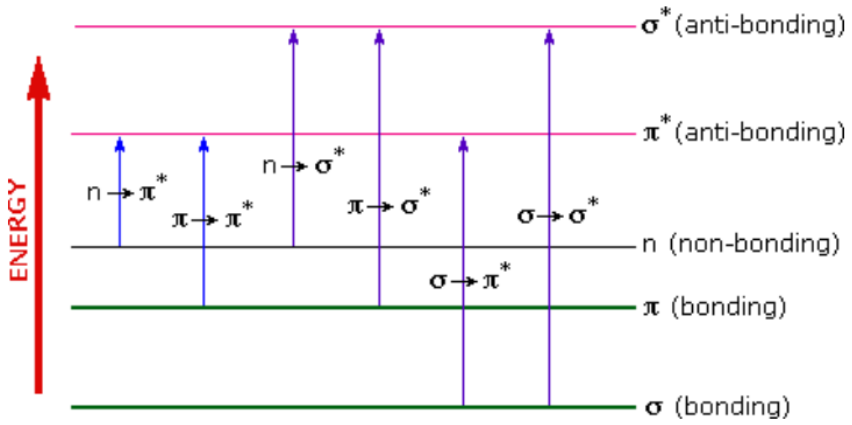

Figure 4-9 Energy levels for electronic transition

When the photon of high energy is absorbed by the electrons in the structure and the electrons jump from valance band to conduction band into the excited state. Only the electrons of specimen whose energies are matching the photons (wavelength) are absorbed which is the unique characteristic of every compound. This is represented by the graph between wavelength

and absorbance or transmittance which further used to calculate band gap by plotting graph using Tauc equation.

$$\epsilon hv = (hv - E_g)^{n}$$

Where,

ε = Absorption

h = Plank's Constant ($6.6026 * 10^{-34}$)

v = frequency

Eg = Band gap

n = ½ for direct and 2 for indirect band gaps

Some more formulas are used for band gap calculations which are

$$A = 2 - log_{10} \%T$$

$$R + T + A = 1$$

$$\alpha = \frac{1}{d} \ln(\frac{1-R^2}{T})$$

Where, R = reflection

A = molar absorptivity

d = film thickness

By using these equations, now the graph between $hv\ vs\ (\alpha hv)^2$ is plotted where the straight line along vertical x-axis is extrapolated to x-axis. This point at gives us the optical band gap of thin films.

4.3.6 I-V Characterization Setup:

The electrochemical setup is used for this purpose. The three electrode system was converted to two electrode system by using working and auxiliary as one and the reference electrode as second one. Reference electrode was connect to cell one with ITO i.e. cathode and the other one with working electrode was attached to the coated cell side i.e. anode. The light source was

set at calibrated distance to give 100mW, the energy of sunlight on clear day. The I-V curves were obtained and further used for calculations of Voc, Jsc, FF and PCE of solar device.

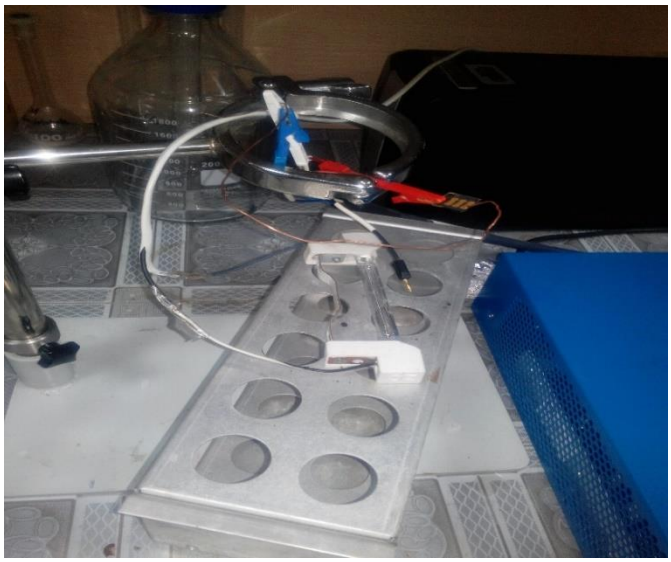

Figure 4-10 Setup for measuring I-V characteristics curve

Chapter 5

Experiment Work

5.1 ZnO Sol Preparation:

ZnO Sol was prepared using Zinc Acetate Dihydrate (ZnAcDH) as precursor, Iso-propanol alcohol as the solvent and Ethanol amine as the stabilizer was added to beaker in below given amount in table 1 for the preparation of 0.4M ZnO sol. It was then stirred until opaque solution turns clear solution i.e. ZnAcDH was completely dissolved. The resultant solution was left for 24 hrs aging.[40]

Table 5-1 ZnO sol composition

Chemicals	**Amount**
Zinc Acetate Dihydrate $(CH3COOH)_2.2H_2O$	4.42 g
Iso-propanol alcohol	50 ml
Ethanol amine	1.207 ml

5.2 Chemicals Used:

Zinc Acetate Dihydrate, (ZnAcDH) by Riedel-deHaen, Ethanol amine (MEA) by Riedel-deHaen, Iso-propanol Alcohol (IPA) by Analar, Molybdenum disulphide (MoS_2), N-Methyl-2-pyrrolidone (NMP). All chemicals used are of analytical grade and are 99.99% pure.

5.3 Molybdenum Disulphide MoS_2:

There are different methods for obtaining the 2D layers of MoS_2, some of them are

- Liquid Phase exfoliation
- Chemical exfoliation
- Micro exfoliation

- Electrochemical exfoliation

Liquid phase exfoliation is used here to get single layer MoS_2 sheets.

5.3.1 Liquid Phase Exfoliation Steps:

In this technique MoS_2 powder is dispersed in the solvent NMP in this case it is 0.1g/ml and is sonicated for 66 hours. The probe sonicator was set at amplitude 60 and frequency 0.6.

The sonication process generates heat which raises the solvent temperature and evaporate it or re-agglomerates the exfoliated MoS_2 sheets. To avoid this chiller is used with water bath which is set at 2^oC which help control solvent temperature. After 66 hours sonication the dispersion was left for 72 hours undisturbed, allowing unexfoliated MoS_2 to settle down under gravity.

5.3.2 Centrifugation:

The solvent was carefully transferred to centrifuge vails and was centrifuged for 90 min at 4000 rpm to get the finest few layer sheets. The supernatant was removed and kept for further process.

5.3.3 Vacuum Filtration:

The dispersion of MoS_2 sheets is in NMP to disperse it in the solvent of desire, the supernatant collected after centrifugation was filtered out over 0.22 um nylon filter paper using filtration assembly attached to vacuum pump. The filter paper was left for air drying.

5.3.4 Dispersion:

The filter paper was bath sonicated for 20 min in Iso-propanol alcohol. The dried filter paper was weigh before and after sonication for determining concertation of the dispersion. Which was diluted to get required 0.01mg/ml of dispersion for further use.

5.3.5 ZnO and MoS_2 Thin films Preparation:

Approach used for making ZnO-MoS_2 composite thin films is by adding MoS_2 dispersed in IPA to ZnO sol in different compositions. After addition of MoS_2 to ZnO sol, the solution was shaken well before spin coating.

Table 5-2 ZnO-MoS_2 sample concentrations

Precursor Composite Sol	**ZnO Sol (ml)**	**MoS_2 in IPA (ml)**	**Vol. % of MoS_2 dispersion**
ZnO pure	1	0	0
ZnO-MoS_2 1	1	0.4	40
ZnO-MoS_2 2	1	0.8	80
ZnO-MoS_2 3	1	1.2	120
ZnO-MoS_2 4	1	1.6	160

5.3.6 Spin Coating:

Spin Coating was done using spin coater at 2500 rpm for 15 seconds and then samples were placed in oven at 200^oC for 10 minutes. This annealing was done to evaporate solvent and remove any residual organic residuals in the layer coated before second coat.[35] The ITO and glass substrate was coated and pre-annealed three times more, finally we have 4 coat ITO and glass slides. The ITOs used for cyclic voltammetry and cell are masked before coating. The four coats are to avoid any pin holes found in less coated slide which could short the final cell.

5.3.7 Post Annealing:

The Aluminium sheet wrap samples are placed in furnace for post annealing at 400^oC for 2hrs at the rate of 10^oC pre minute heating rate. At 400^oC the organic matter present in films is combusted and crystallization of ZnO occurs.[35]

5.4 Cell Fabrication:

5.4.1 Active Layer Preparation:

P_3HT (Mark lisicon SP001)/ PCBM (Ossila) were mixed in 1:0.8 ratio and dissolved in 0.5ml Chlorobenzene as solvent to form a homogenous solution. The homogenous solution was achieve by magnetically stirring for 24 hours at room.

5.4.2 Preparing ITOs for Device Fabrication:

ITOs coated slide were first sonicated in detergent for 10 mins, then sonicated with deionized water followed by acetone and at last in iso-propanol for 10 mins each. The ITO coated slides are dried in oven and placed in dust and moisture free desiccator until used. The final efficiency of device and smooth coating greatly depends upon the dry, dust free and defect free ITO coated slides.

5.4.3 Cell Fabrication Steps:

First step in synthesis of cell was coating of ZnO and ZnO-MoS_2 over ITO coated slides at 2500 rpm for 15s followed by 10 min heating for dry the film. ITO coated slides were masked before coating. This coating and heating were repeated to gain 4 coats over slides. The coated ITO coated slides were annealed for 2 hr at 400^{o}C.

Annealed slides were ready for coating of active layer over electron transport layer. P3HT/PCBM homogeneous solution was spin coated at 3000 rpm for 30 s, excess solution on side parts of substrate was cleaned by Chlorobenzene. The substrate was place over hot plate at 90^{o}C for 10 min to remove the stresses.

Next step was to coat hole transport layer (HTL) onto the previously coated substrate having ZnO and active layer, PCBM was used as HTL. PCBM was spin coated at 5000rpm for 30 secs, excess PCBM was clean by Chlorobenzene from the substrate. The substrate was placed over hot plate at 90^{o}C for 10 minutes.

Next step inline was to deposit the electrode on to top of coated ITO coated slides by evaporating. Each of ITO coated with active material was placed in masks which are made of Aluminium.

a)  b) 

Figure 5-1 Aluminum masks for electrode deposition b) Finished OPV device

Chapter 6

Results and Discussion

6.1 Molybdenum Disulphide (MoS_2) Characterization:

6.1.1 Scanning Electron Microscope (SEM):

SEM specimen was prepared from the diluted MoS_2 by drop casting on silica substrate. Figure 6.1 shows the single layer Molybdenum disulphide after successful liquid phase exfoliation. MoS_2 over silica substrate shows with many small dispersed flakes and layer structures. The individual (single or multi-layer) sheets shows that exfoliation of MoS_2 powder has been done successfully.

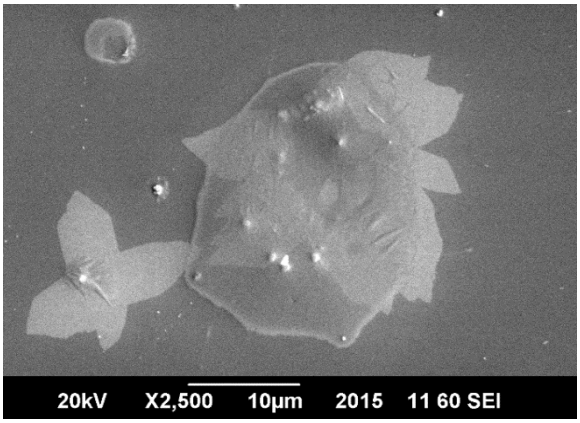

Figure 6-1Sheet of MoS2 at X2500

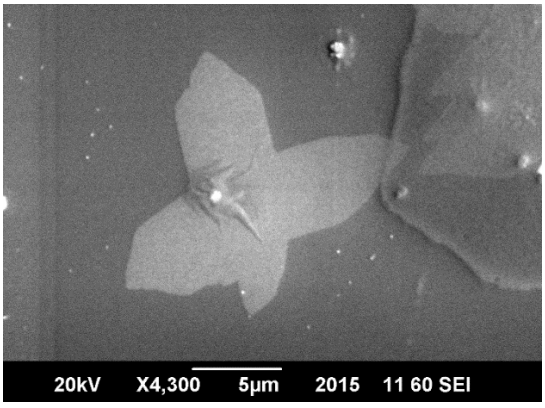

Figure 6-2Sheet of MoS2 at X4300

6.1.2 Atomic Force Microscopy (AFM) of Exfoliated MoS_2:

AFM specimen was prepared by drop casting diluted dispersion of exfoliated MoS_2 over a silica substrate. Figure 6.2 shows the monolayer MoS_2 sheet with thickness of 0.939 nm which shows the successful liquid phase exfoliation of MoS_2 powder. The sheet is almost 186 nm in length which varies at different spots. Presence of monolayers in the dispersion will intern enhance the electrical properties many folds.

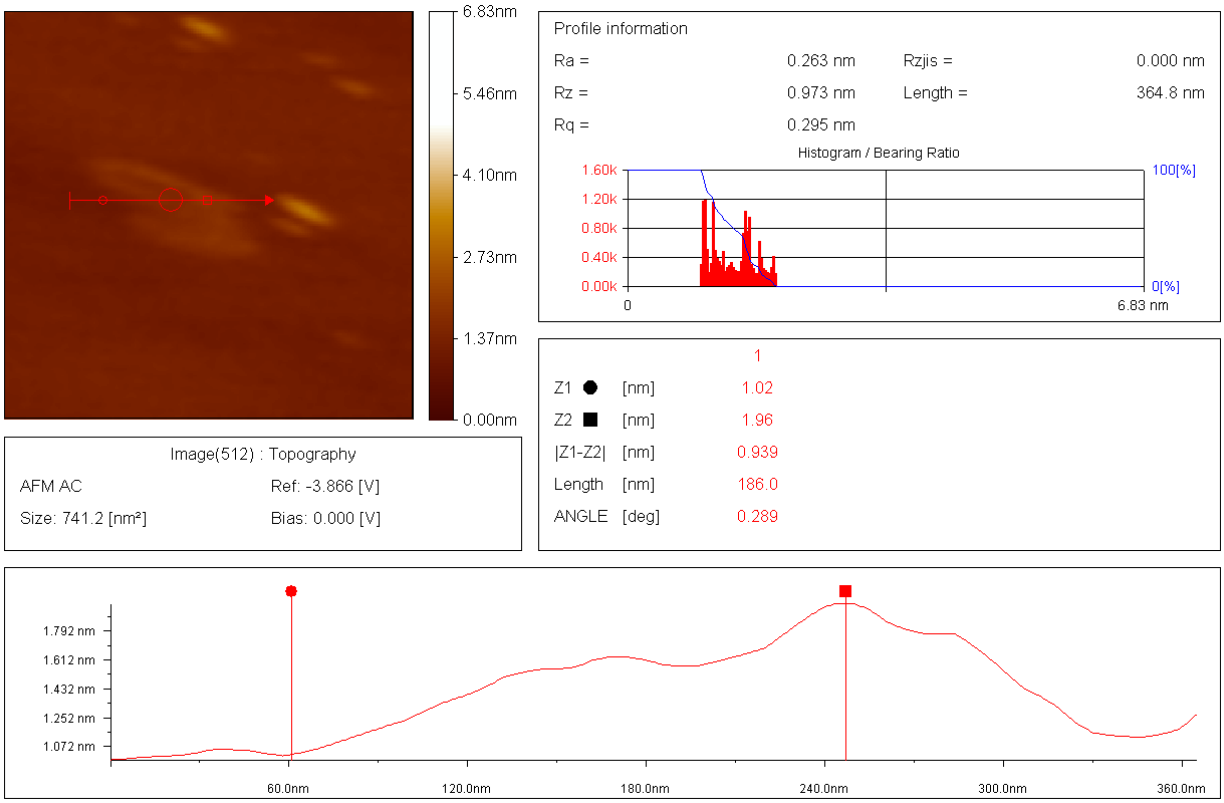

Figure 6-3 Height profile of AFM image of MoS_2 sheet

Image(512) : Topography
741.2 x 741.2 x 6.83 nm

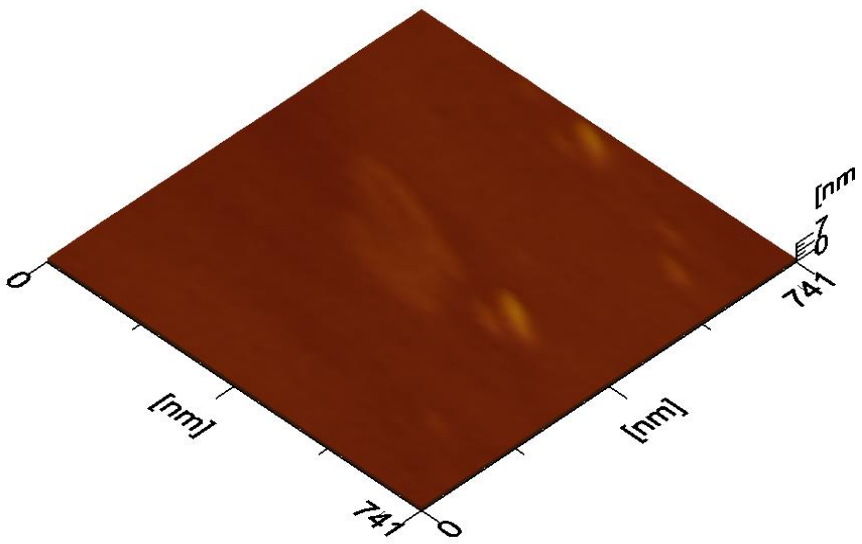

Figure 6-4 Top view in AFM image of MoS_2 thin layer

6.2 ZnO & ZnO-MoS_2 Composite Thin Film Characterization:

The samples of ZnO thin films and ZnO/MoS_2 composite thin films were prepared by spin coating sol on the glass substrate followed by annealing at 400^oC in heating furnace for 2hours. Figure 6-3 shows the image of ZnO nanostructures and nano particles. The images represent homogenously distributed nanostructures and nanoparticles in the range of 13nm – 22nm**.**

6.2.1 Scanning Electron Microscope (SEM) ZnO Thin Film:

ZnO nanoparticle dispersed over the entire glass substrate can be seen. These nanoparticles are homogeneously formed and are of average 16nm. These spherical nano particles from SEM images are in synchronization with the particles from AFM images of identical thin film samples.

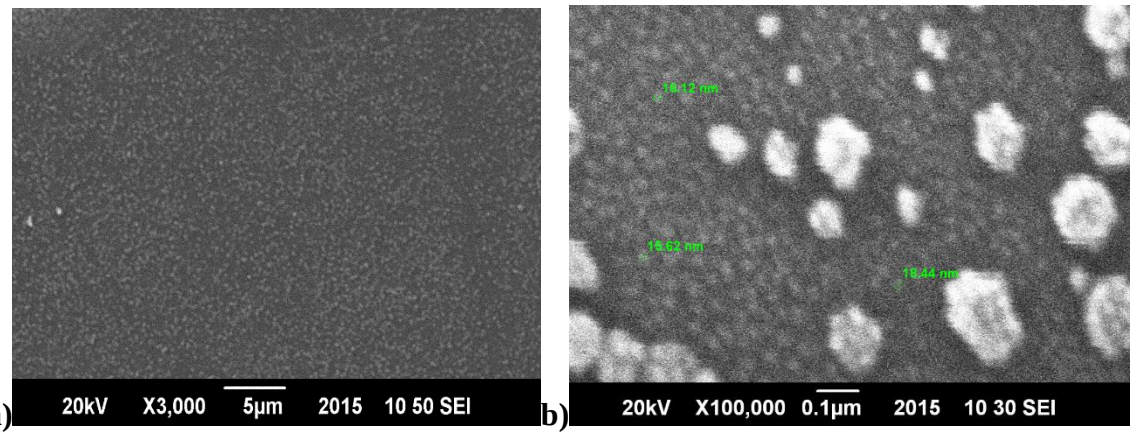

Figure 6-5 ZnO nanoparticles in thin films images of SEM at magnification a) X3000,

b) X100000

Very fine ZnO particles in background can been seen, these nanoparticles are in the range from 15-18 nm in size. These nanoparticles are homogeneously spread over the substrate by spin coating leaving no pinholes in it for the leakage of current.

6.2.2 Atomic Force Microscopy (AFM) of ZnO Thin Film:

AFM specimen was prepared by spin coating ZnO and ZnO-MoS_2 composite thin film over clean glass slides by following steps in the section 5.4 of previous chapter. 2 coat and 4 coat samples are prepared for study using AFM. As from Figure 6.- the substrate with ZnO 2 coats have left pin hole in the film, which could short if 2 coat film coats are used in cell fabrication that's why 4 coat ZnO and ZnO-MoS_2 thin film are used in this study.

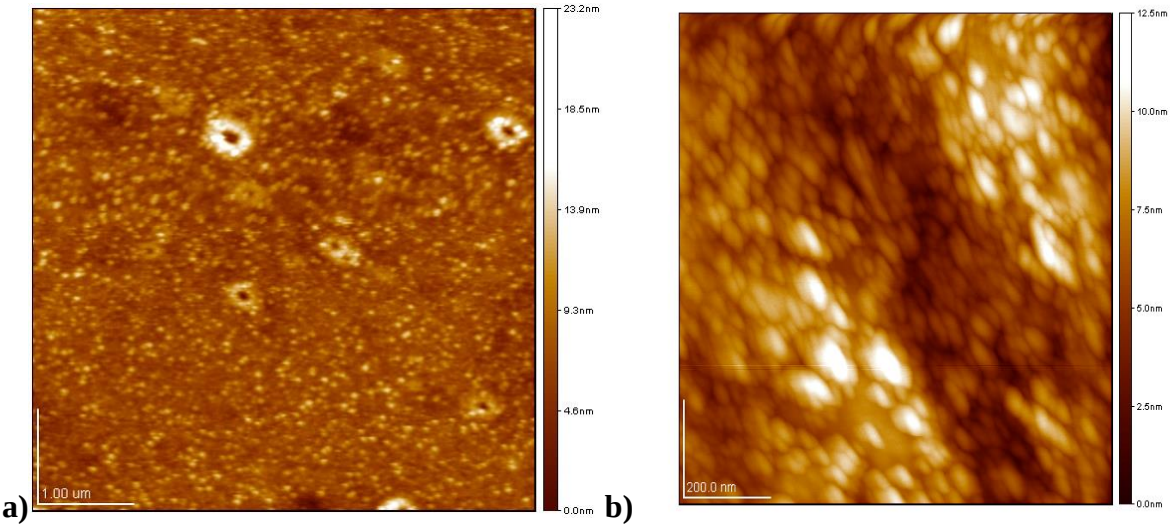

a) **b)**

Figure 6-6 AFM image ZnO thin film with a) two coats and b) four coats

Figure 6.5 a shows ZnO nanoparticles are distributed homogeneously over the glass substrate. This thin film is covering whole area leaving no area for shortening of circuit. It shows that the substrate with ZnO 4 coats and annealed is more homogeneous and pin hole free which is better for further use in device fabrication. The 3D topography also confirms the homogeneity and fine nanoparticles spread in ZnO thin film which is coated 4 times.

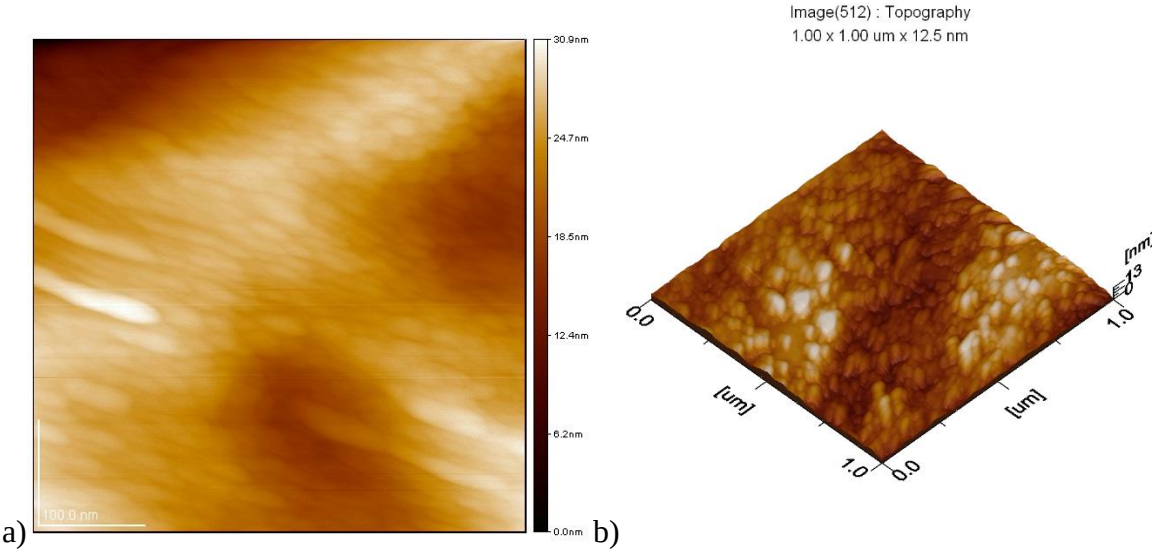

a) b)

Figure 6-7 AFM image of ZnO nano particles a) in thin film b) in top view image

6.3 X-ray Diffraction (XRD) of ZnO and MoS_2:

XRD results exfoliated MoS_2 and ZnO thin film shows the presence of required peaks in the figures.

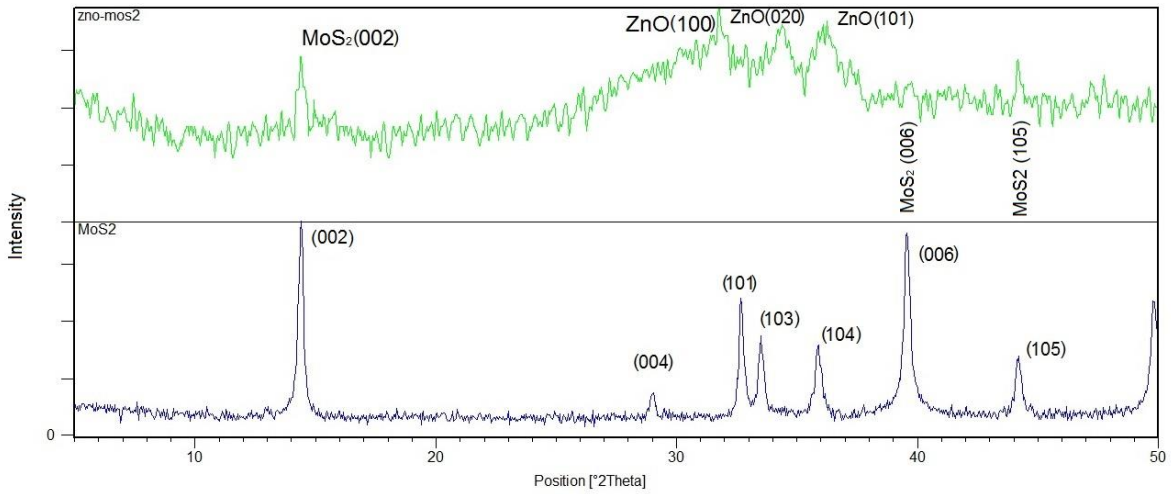

Figure 6-8 XRD for ZnO-MoS_2 thin film and exfoliated MoS_2

Figure 6.9 shows the peaks of ZnO at 2 theta value of 32 have plane 100, at theta 34 having 002 and 36 theta 101 are same as found in literature.[40] The the peak from experimental MoS_2 resembles the peaks given in literature.[41] Peak of 002 MoS2 at 14.8 is found in literature along with others. In ZnO-MoS_2 concentration XRD result, the ZnO peaks in region 2 theta 30-40 are prominent which are comparable to one in literature but MoS_2 peaks are suppressed.

6.4 Band Gap Analysis by UV-VIS Spectroscopy:

Following graphs are plotted by Tauc equation as discussed earlier in section 4.3.2 using wavelength, absorbance and film thickness

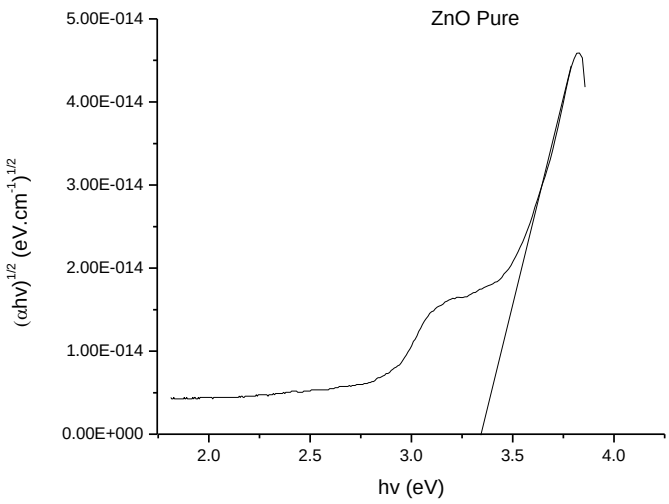

a)

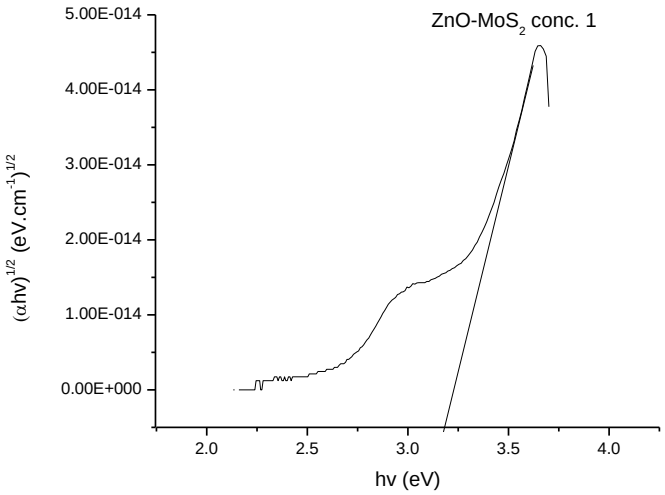
ZnO-MoS2 conc. 1
5.00E-014
4.00E-014
3.00E-014
2.00E-014
1.00E-014
0.00E+000
(αhv)1/2 (eV.cm-1)1/2
2.0
2.5
3.0
3.5
4.0
hv (eV)

b)

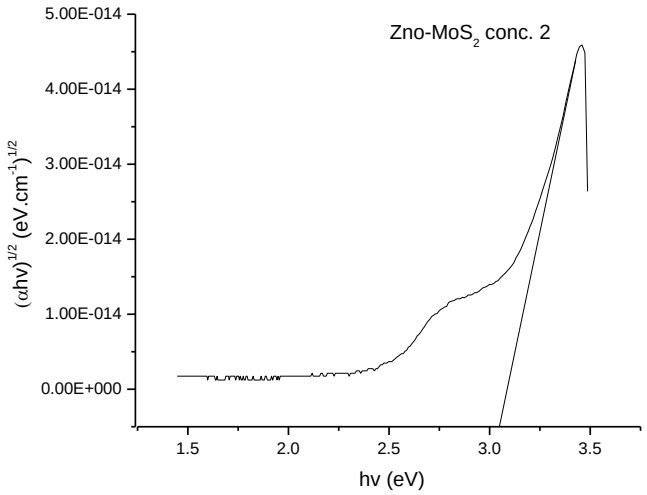
Zno-MoS2 conc. 2
5.00E-014
4.00E-014
3.00E-014
2.00E-014
1.00E-014
0.00E+000
(αhv)1/2 (eV.cm-1)1/2
1.5
2.0
2.5
3.0
3.5
hv (eV)

c)

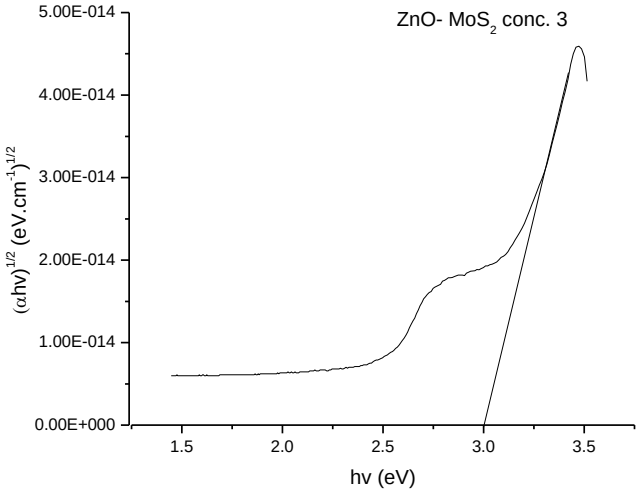
ZnO- MoS2 conc. 3
5.00E-014
4.00E-014
3.00E-014
2.00E-014
1.00E-014
0.00E+000
(αhv)1/2 (eV.cm-1)1/2
1.5
2.0
2.5
3.0
3.5
hv (eV)

d)

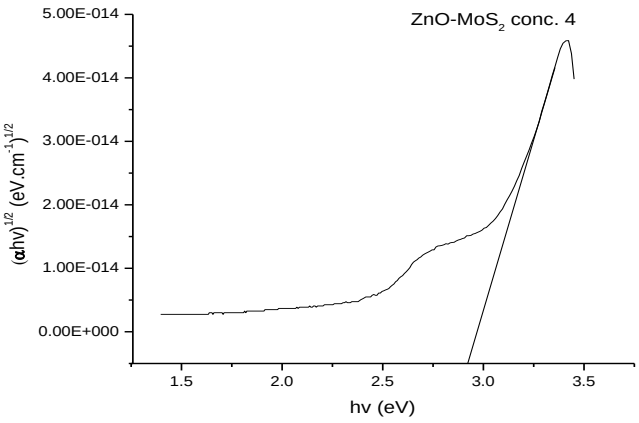

e)

Figure 6-9 Curves form data used from UV Vis data in a, b, c, d, e

Table 6-1 Band gap from UV VIS spectroscopy

Thin film composition	Band gap
ZnO pure	3.34
ZnO-MoS_2 1	3.18
ZnO-MoS_2 2	3.04
ZnO-MoS_2 3	3.00
ZnO-MoS_2 4	2.92

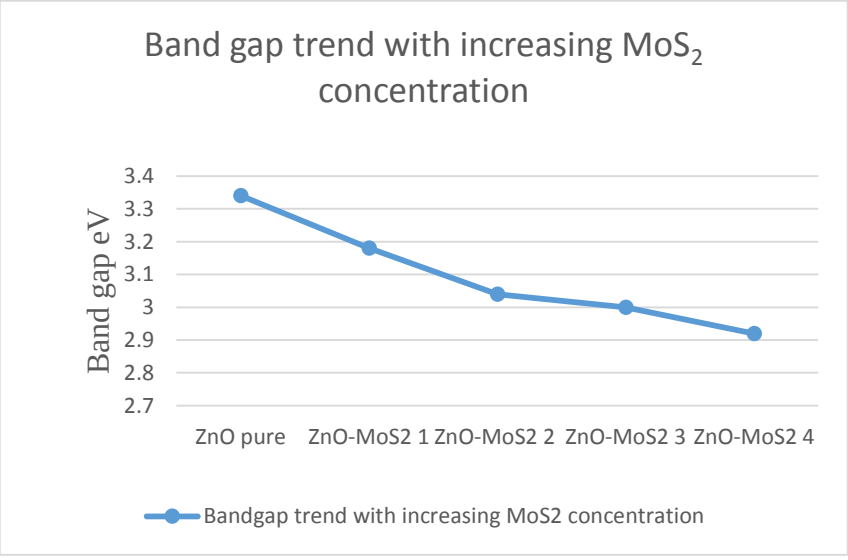

Figure 6-10 ZnO compositions vs Band gap

Discussion:

The results plotted in Figure 6-6 shows the band gap reduction of ZnO thin film with increasing concentration of MoS_2 which supports our hypothesis about 2D material added. This means its absorption is shifted to higher wavelengths in visible region.

6.5 Band Gap Analysis by Cyclic Voltammetry (CV):

Band gap of pure ZnO and different ZnO-MoS_2 concentrations coated on ITO coated glass were calculated using information from below graphs.

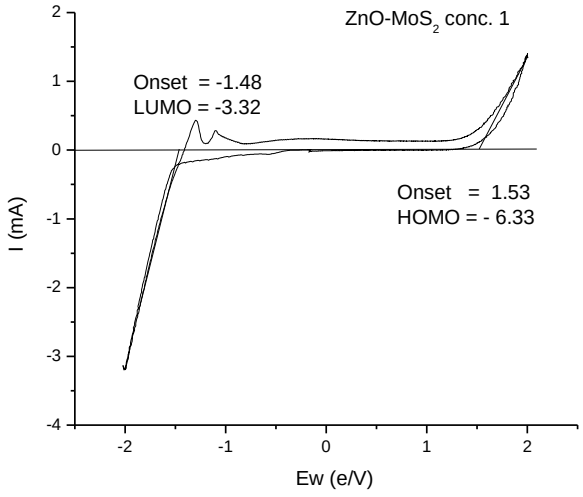

a)

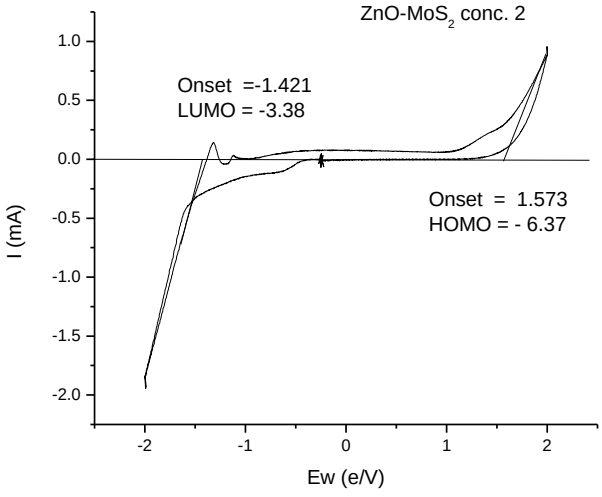

b)

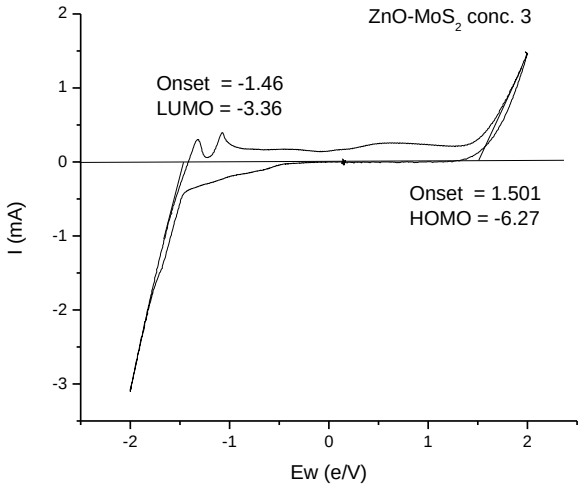

c)

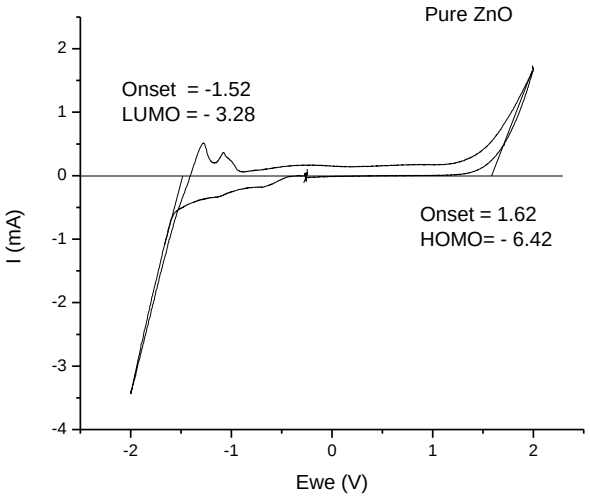

d)

Figure 6-11 E vs I curves for band gap calculations from a, b, c, d

From all of above graph HOMO, LUMO and band gap is measured by using the given formulas as mentioned below,

$E_{HOMO} = E_{onset} - 4.8$

$E_{LUMO} = E_{onset} - 4.8$

$E_{Band\ gap} = E_{HOMO} - E_{LUMO}$

Table 6-2 HOMO, LUMO and Band gap of different compositions.

Film Concentration	HOMO	LUMO	Band gap eV
ZnO pure	-6.42	-3.28	3.14
ZnO-MoS_2 1	-6.33	-3.32	3.01
ZnO-MoS_2 2	-6.37	-3.38	2.99
ZnO-MoS_2 3	-6.27	-3.36	2.91
ZnO-MoS_2 4	-6.27	-3.38	2.89

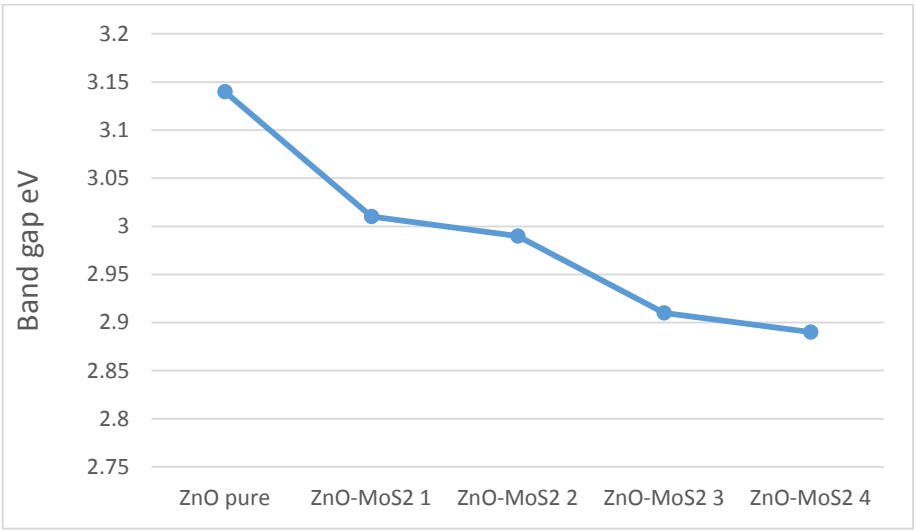

Figure 6-12 Band gap trend with increasing concentration of MoS_2 in ZnO

6.5.1 Discussion:

The results from UV-VIS spectroscopy and CV confirmed the reduction in band gap as the concentration of MoS_2 is increasing in ZnO thin films. In case of CV pure ZnO thin film shows the band gap of 3.04 which on addition of MoS_2 starts decreasing and ZnO-MoS_2 4 shows the highest reduction in band gap i.e. 2.89. This reduction in band gap enhances the photo response of ZnO thin films in noticeable area. Due to enhanced electrical conductivity and electron transfer of the exfoliated monolayer MoS_2, it provides better electron transport from the conduction band and hence lowering the probability of recombination of electron hole.

6.6 Characterization of Hybrid Solar Device:

6.6.1 I-V Characteristics of Devices:

Electrochemical chemical spectroscopy was used for this purpose, the I-V curves of ZnO and ZnO-MoS_2 concentrations are:

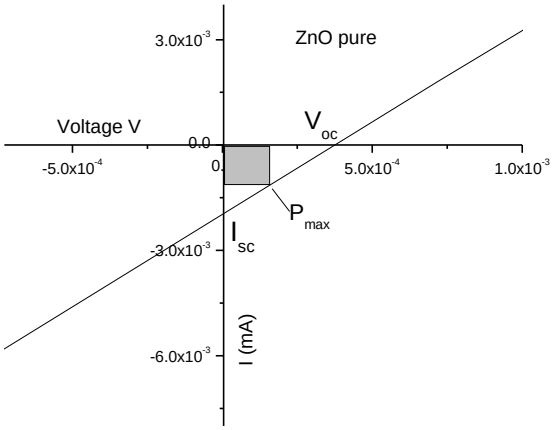

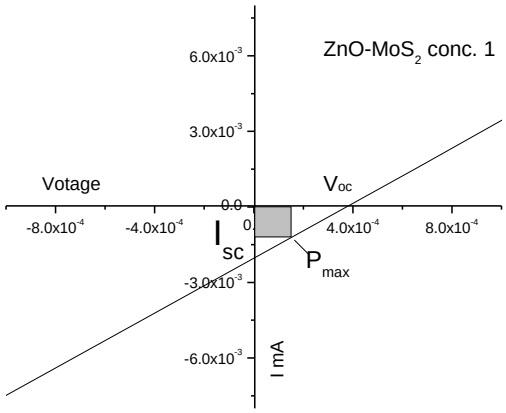

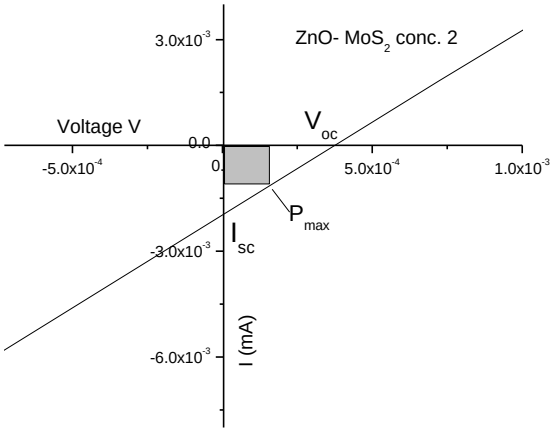

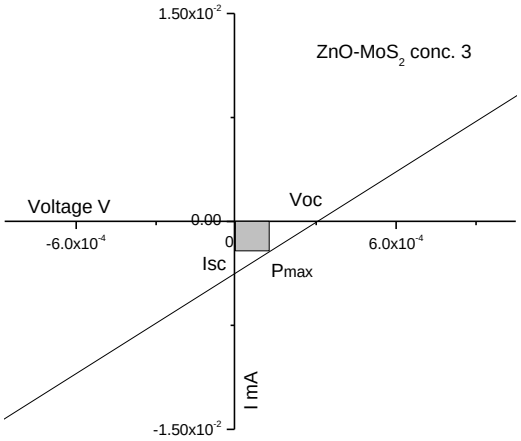

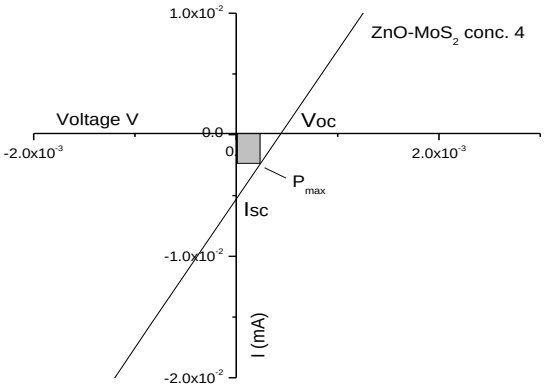

Figure 6-13 I-V Characteristic curves for different compositions.

Table 6-3 Values from I-V characteristics curves of different devices

Composition	**Isc (µA)**	**V (mV)**	**Im (µA)**	**Vm (mA)**	**Fill Factor**
ZnO pure	1.98	3.74E-01	1.10	1.60E-01	0.231
ZnO-MoS_2 1	2.04	3.80E-01	1.2	1.50E-01	0.232
ZnO-MoS_2 2	2.38	2.99E-02	1.31	1.30E-02	0.238
ZnO-MoS_2 3	3.7	3.04E-01	2.21	1.23E-01	0.241
ZnO-MoS_2 4	5.0	4.52E-01	2.35	2.34E-01	0.243

Figure 6-14 Increasing trend in Isc with increasing MoS2 concentration

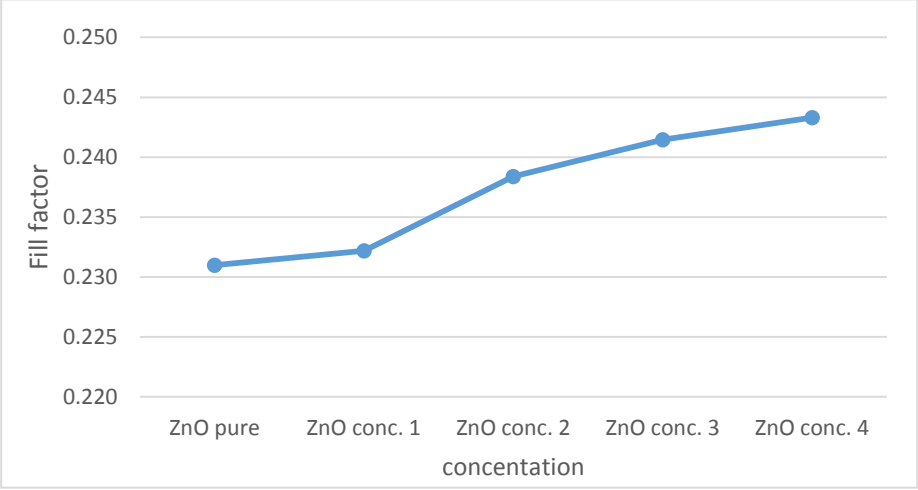

Figure 6-15 Increase in fill factor with increasing MoS_2 concentration in ZnO

Area of device is 0.8cm^{-2} and the illuminating source is set at 100 mW/cm^{-2} which is equals to sunlight on clear day.

Table 6-4 Comparison of concentration, Jsc and Pr

Concentration	Jsc (µA/cm^2)	Parasitic Resistance (Pr)
ZnO pure	2.49	1.69E-01
ZnO-MoS_2 1	2.55	1.68E-01
ZnO-MoS_2 2	2.98	1.13E-02
ZnO-MoS_2 3	4.62	7.39E-02
ZnO-MoS_2 4	6.25	8.14E-02

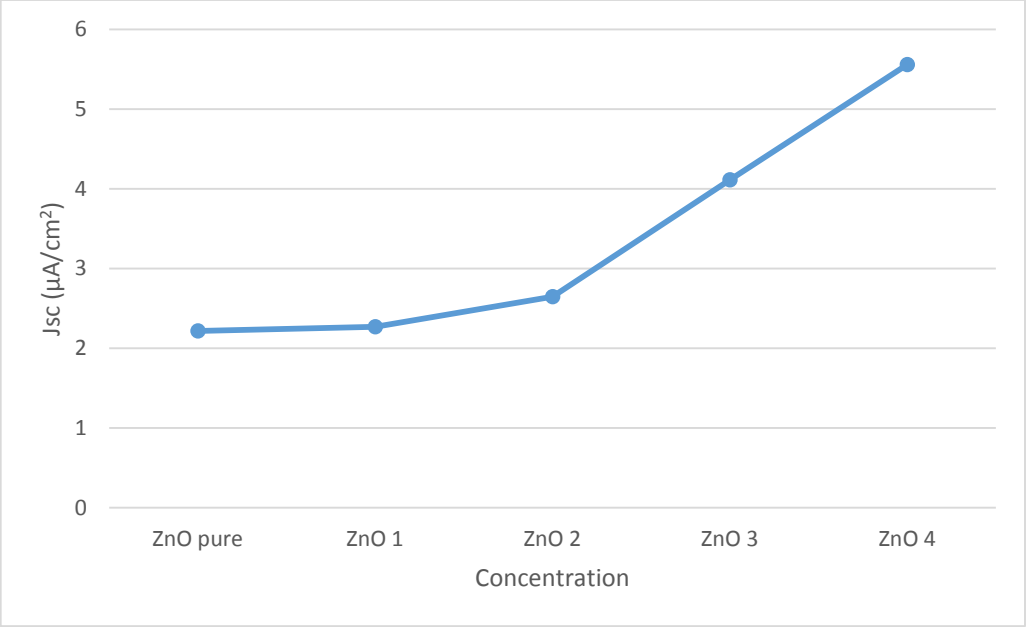

Figure 6-16 Increasing trend in Jsc with increasing MoS_2 concentration

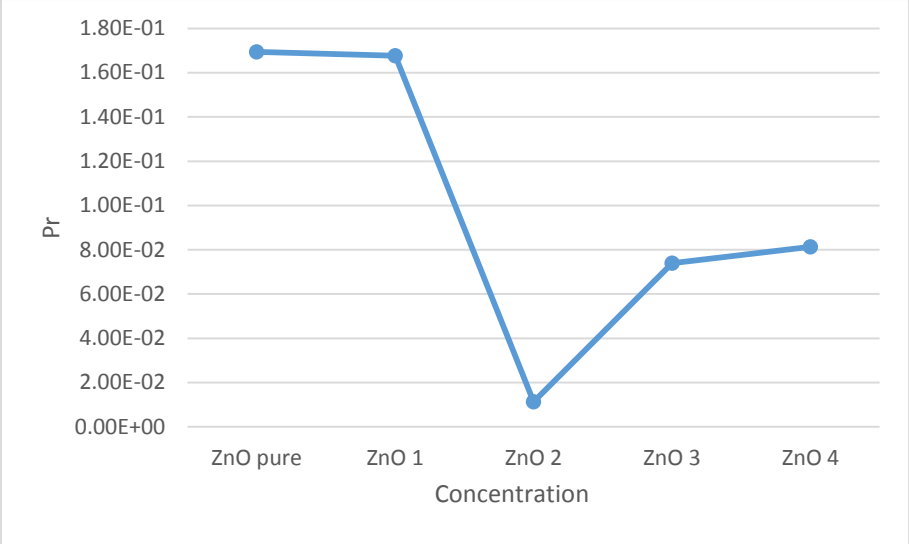

Figure 6-17 Decreasing parasitic resistance with MoS_2 concentration

6.6.2 Discussion:

The overall increase in fill factor was noted as the concentration of MoS_2 was raised in ZnO which means that MoS_2 nano sheet due to their superior charge mobility and charge transfer was acting as bridge between the ZnO layer and ITO.

Fill factor is the ratio of P_{max} (theoretical) and P_{out} (actual) which means it's always less than equal to one (ideal). Higher fill factors means the actual P_{out} is reaching near to theoretical maximum power which there are less parasitic resistance losses in the device, and low FF mean that the parasitic resistance is high i.e. Shunt and series resistance in cell are effective. Low FF also means low shunt and high series resistance. Shunt resistance effects the Isc by providing alternating route for current and increase in series resistance decreases Voc due to resistance between contacts.

Increasing trend in current Isc in figure 6-15 with increasing MoS_2 concentration in ZnO thin film, is due to the electron mobility of 2D material which has increased the electrons flow to the cathode which in return increasing the overall current of the device.

Parasitic resistance is also decreasing which means the series resistance in the circuit is reduced, which means the resistance between contacts of layer is decreased. Decreasing parasitic resistance also indicates the effect of shunt resistance is changed for good i.e. current flowing through alternating routes is decreased due to inclusion of MoS_2 in ZnO.

Energy band gap in inverted photovoltaic cell model is given by the following schematic.

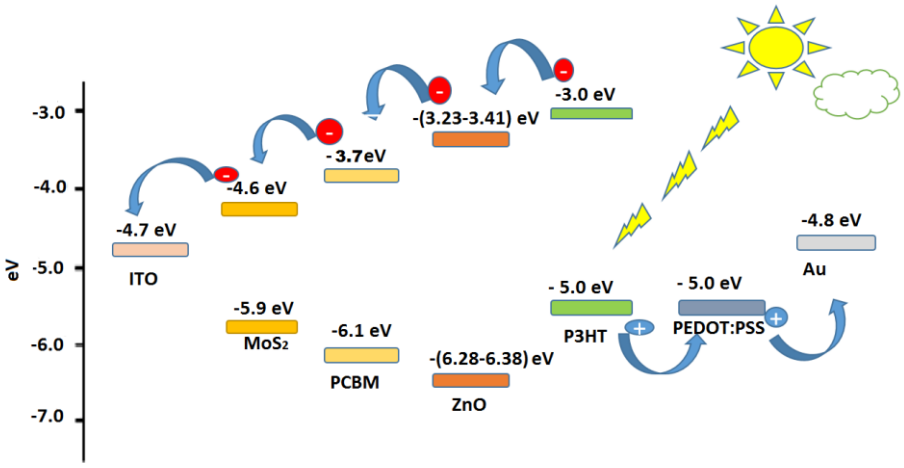

Figure 6-18 Schematic of energy band diagram of inverted OPV device

In figure 6-10, P3HT is acting as donor material, while ZnO-MoS_2 as electron transport layer and PCBM is acting as electron acceptor material, ITO is acting as cathode. PEDOT:PSS is acting as hole transport layer and gold as its anode. The electron-hole pairs are dissociated at interface between P3HT and PCBM, from where electrons moves to the electron transport material and then to cathode. From the schematic the generation of charges and the movement of electrons from the LUMO level of ZnO to LUMO of MOS_2 and finally to ITO can be seen. While the hole is transported from the HOMO level of P3HT to HOMO of PEDOT:PSS and then to Au.

Chapter 7

Conclusion:

ZnO thin films with homogeneous nano particles in range of 15-17nm are fabricated and the number of coats are optimized to four as less would have more probability of pin holes in it.

Using liquid exfoliated technique, monolayer MoS_2 was successfully produced, which give very fine dispersion for further use. The images of exfoliated MoS_2 from AFM showing MoS_2 sheet of about 0.939 nm thickness and SEM images also approves the successful exfoliation.

Exfoliated MoS_2 is successfully used with ZnO for the reduction of band gap, which the cyclic voltammetry records show to be minimum of 2.90 eV for the 160% by volume concentration of MoS_2 in ZnO-MoS_2 thin. The results from UV-VIS spectroscopy also approves of this reduction.

Inverted photovoltaic devices are fabricated using ZnO-MoS_2 different concertation, I-V characteristics of cell showing that with increasing MoS_2 concentration the fill factor, current Isc and current density Jsc is increasing which is due to decrease in the parasitic resistance. It means that ZnO thin films with MoS_2 in it has better photo response and electron mobility properties.

7.1 Future work:

- To study electronic properties of ZnO-MoS_2 composite at varying temperatures conditions with different techniques.
- Use of different active layer materials with ZnO-MoS_2 composite for enhancing overall efficiency in photovoltaic devices.
- To investigate the effect on band gap of ZnO thin film by inclusion of MoS_2 sheets at varying centrifuging speeds like 1000,2000 and 3000 rpm.
- To investigate different Metal oxide and study the changes in band gaps and other properties with inclusion of 2D materials.

Reference:

[1] "Renewables 2015 Global Status Report", Renewable Energy Policy Network for the 21st Century, pp. 5-9, 2015.

[2] F. C. Krebs, M. Hösel, M. Corazza, B. Roth, M. V. Madsen, S. A. Gevorgyan, *et al.*, "Freely available OPV-The fast way to progress," *Energy Technology*, vol. 1, pp. 378-381, 2013.

[3] G. Conibeer, M. Green, R. Corkish, Y. Cho, E.-C. Cho, C.-W. Jiang, et al., "Silicon nanostructures for third generation photovoltaic solar cells," Thin Solid Films, vol. 511-512, pp. 654-662, 2006.

[4] Y. Zhou, M. Eck, and M. Krüger, Organic-Inorganic Hybrid Solar Cells: State of the Art, Challenges and Perspectives: INTECH Open Access Publisher, 2011.

[5] H. Lund, R. Nilsen, O. Salomatova, D. Skåre, and E. Riisem. "Different generations of solar cells", 2015

[6] K. D. Jayawardena, L. J. Rozanski, C. A. Mills, M. J. Beliatis, N. A. Nismy, and S. R. Silva, "'Inorganics-in-organics': recent developments and outlook for 4G polymer solar cells," Nanoscale, vol. 5, pp. 8411-27, 2013.

[7] B. R. Saunders, "Hybrid polymer/nanoparticle solar cells: preparation, principles and challenges," J Colloid Interface Sci, vol. 369, pp. 1-15, 2012.

[8] J. D. Kotlarski and P. W. M. Blom, "Impact of unbalanced charge transport on the efficiency of normal and inverted solar cells," Applied Physics Letters, vol. 100, pp. 013306, 2012.

[9] T. L. Benanti and D. Venkataraman, "Organic solar cells: an overview focusing on active layer morphology," Photosynth Res, vol. 87, pp. 73-81, 2006.

[10] M. Wright and A. Uddin, "Organic-inorganic hybrid solar cells: A comparative review," Solar Energy Materials and Solar Cells, vol. 107, pp. 87-111, 2012.

[11] M. C. Scharber, D. Mühlbacher, M. Koppe, P. Denk, C. Waldauf, A. J. Heeger, et al., "Design Rules for Donors in Bulk-Heterojunction Solar Cells—Towards 10 % Energy-Conversion Efficiency," Advanced Materials, vol. 18, pp. 789-794, 2006.

[12] G. Yu, J. Gao, J. C. Hummelen, F. Wudl, and A. J. Heeger, "Polymer Photovoltaic Cells: Enhanced Efficiencies via a Network of Internal Donor-Acceptor Heterojunctions," SCIENCE, vol. 270, 1995.

[13] J. Nelson, "Organic photovoltaic films," Current Opinion in Solid State and Materials Science, vol. 6, pp. 87-95, 2002.

[14] Y. J. Cheng, S. H. Yang, and C. S. Hsu, "Synthesis of conjugated polymers for organic solar cell applications," *Chem Rev*, vol. 109, pp. 5868-923, 2009.

[15] S. Emin, S. P. Singh, L. Han, N. Satoh, and A. Islam, "Colloidal quantum dot solar cells," Solar Energy, vol. 85, pp. 1264-1282, 2011.

[16] T.-Y. Chu, J. Lu, S. Beaupré, Y. Zhang, J.-R. Pouliot, S. Wakim, *et al.*, "Bulk heterojunction solar cells using thieno [3, 4-c] pyrrole-4, 6-dione and dithieno [3, 2-b: 2′, 3′-d] silole copolymer with a power conversion efficiency of 7.3%," *Journal of the American Chemical Society*, vol. 133, pp. 4250-4253, 2011.

[17] C. J. Brabe, A. Cravino, D. Meissner, N. S. Sariciftci, T. Fromherz, M. T. Rispens, et al., "Origin of the Open Circuit Voltage of Plastic Solar Cells," Advanced Functional Materials, vol. 11, 2001.

[18] A. Xie and Aozhen,"Exfoliation of transitional metal dichalogenides (TMDS) and the Application of co-Exfolation of MoS_2/Natural Graphite in Lithium Ion Battery (LIB)," Master of Science, University of Akron, 2014.

[19] S. Lattante, "Electron and Hole Transport Layers: Their Use in Inverted Bulk Heterojunction Polymer Solar Cells," Electronics, vol. 3, pp. 132-164, 2014.

[20] X. Yang, J. Loos, S. C. Veenstra, W. J. Verhees, M. M. Wienk, J. M. Kroon, et al., "Nanoscale morphology of high-performance polymer solar cells," Nano Lett, vol. 5, pp. 579-83, 2005.

[21] Y. Liang, Z. Xu, J. Xia, S. T. Tsai, Y. Wu, G. Li, et al., "For the bright future-bulk heterojunction polymer solar cells with power conversion efficiency of 7.4%," Adv Mater, vol. 22, pp. E135-8, 2010.

[22] H. Borchert, "Elementary processes and limiting factors in hybrid polymer/nanoparticle solar cells," Energy & Environmental Science, vol. 3, pp. 1682, 2010.

[23] X. Yang and A. Uddin, "RETRACTED: Effect of thermal annealing on P3HT:PCBM bulk-heterojunction organic solar cells: A critical review," Renewable and sustainable Energy Reviews, vol. 30, pp. 324-336, 2014.

[24] J. Weickert, R. B. Dunbar, H. C. Hesse, W. Wiedemann, and L. Schmidt-Mende, "Nanostructured organic and hybrid solar cells," Adv Mater, vol. 23, pp. 1810-28, 2011.

[25] T.-H. Lai, S.-W. Tsang, J. R. Manders, S. Chen, and F. So, "Properties of interlayer for organic photovoltaics," Materials Today, vol. 16, pp. 424-432, 2013.

[26] J.-H. Lee, K.-H. Ko, and B.-O. Park, "Electrical and optical properties of ZnO transparent conducting films by the sol–gel method," Journal of Crystal Growth, vol. 247, pp. 119-125, 2003.

[27] Z. L. Wang, "Nanostructures of zinc oxide," Materials Today, vol. 7, pp. 26-33, 2004.

[28] Z. L. Wang, "Zinc oxide nanostructures: growth, properties and applications," Journal of Physics: Condensed Matter, vol. 16, pp. R829, 2004.

[29] Q. H. Wang, K. Kalantar-Zadeh, A. Kis, J. N. Coleman, and M. S. Strano, "Electronics and optoelectronics of two-dimensional transition metal dichalcogenides," Nature Nanotechnology, vol. 7, pp. 699-712, 2012.

[30] A. Winchester, S. Ghosh, S. Feng, A. L. Elias, T. Mallouk, M. Terrones, et al., "Electrochemical Characterization of Liquid Phase Exfoliated Two-Dimensional Layers of Molybdenum Disulfide," ACS Applied Materials & Interfaces, vol. 6, pp. 2125-2130, 2014.

[31] J. V. Lauritsen, J. Kibsgaard, S. Helveg, H. Topsoe, B. S. Clausen, E. Laegsgaard, et al., "Size-dependent structure of MoS2 nanocrystals," Nature Nanotechnology, vol. 2, pp. 53-8, 2007.

[32] K. F. Mak, C. Lee, J. Hone, J. Shan, and T. F. Heinz, "Atomically ThinMoS2: A New Direct-Gap Semiconductor," Physical Review Letters, vol. 105, 2010.

[33] A. Splendiani, L. Sun, Y. Zhang, T. Li, J. Kim, C.-Y. Chim, et al., "Emerging Photoluminescence in Monolayer MoS2," Nano Letters, vol. 10, pp. 1271-1275, 2010.

[34] M. Bernardi, M. Palummo, and J. C. Grossman, "Extraordinary Sunlight Absorption and One Nanometer Thick Photovoltaics Using Two-Dimensional Monolayer Materials," Nano Letters, vol. 13, pp. 3664-3670, 2013.

[35] A. Kołodziejczak-Radzimska and T. Jesionowski, "Zinc Oxide—From Synthesis to Application: A Review," Materials, vol. 7, pp. 2833-2881, 2014.

[36] J. Lee, A. J. Easteal, U. Pal, and D. Bhattacharyya, "Evolution of ZnO nanostructures in sol–gel synthesis," Current Applied Physics, vol. 9, pp. 792-796, 2009.

[37] K. L. Foo, M. Kashif, U. Hashim, and M. E. Ali, "Fabrication and Characterization of ZnO Thin Films by Sol-Gel Spin Coating Method for the Determination of Phosphate Buffer Saline Concentration," Current Nanoscience, vol. 9, pp. 288-292, 2013.

[38] N. A. Burnham, F. Cruceanu, Q. Dong, and N. P. Thompson. "An Introduction to Atomic Force Microscopy", 2015.

[39] J. Heinze, "Cyclic Voltammetry—“Electrochemical Spectroscopy”. New Analytical Methods(25)," Angewandte Chemie International Edition in English, vol. 23, pp. 831-847, 1984.

[40] S. Salam, M. Islam, and A. Akram, "Sol–gel synthesis of intrinsic and aluminum-doped zinc oxide thin films as transparent conducting oxides for thin film solar cells," Thin Solid Films, vol. 529, pp. 242-247, 2013.

[41] B. Visic, R. Dominko, M. K. Gunde, N. Hauptman, S. D. Skapin, and M. Remskar, "Optical properties of exfoliated MoS2 coaxial nanotubes - analogues of graphene," Nanoscale Res Lett, vol. 6, pp. 593, 2011.